

AD-A254 577

SECUR



DISTRIBUTION STATEMENT A

Approved for public release
Distribution Unlimited

②

RT DOCUMENTATION PAGE

DTIC
SELECTED
AUG 17 1992
S-1

1a. REPORT SECURITY CLASSIFICATION Unclassified			1b. RESTRICTIVE MARKINGS	
2a. SECURITY CLASSIFICATION AUTHORITY			3. DISTRIBUTION/AVAILABILITY OF REPORT Unlimited	
2b. DECLASSIFICATION/DOWNGRADING SCHEDULE			5. MONITORING ORGANIZATION REPORT NUMBER(S)	
4. PERFORMING ORGANIZATION REPORT NUMBER(S) Annual Report 1991-1992			7a. NAME OF MONITORING ORGANIZATION	
6a. NAME OF PERFORMING ORGANIZATION Univ. of California, San Diego		6b. OFFICE SYMBOL (if applicable)	7b. ADDRESS (City, State, and ZIP Code) Univ. of California, San Diego (A-034) 8603 La Jolla Shores Dr. La Jolla, CA 92093-0234	
6c. ADDRESS (City, State, and ZIP Code) Electrical & Computer Engineering Dept. 0407 La Jolla, CA 92093-0407		9. PROCUREMENT INSTRUMENT IDENTIFICATION NUMBER N00014-91-K-2019		
8a. NAME OF FUNDING/SPONSORING ORGANIZATION Naval Research Laboratory	8b. OFFICE SYMBOL (if applicable) code N00173	10. SOURCE OF FUNDING NUMBERS		
8c. ADDRESS (City, State, and ZIP Code) 4555 Overlook Ave., S.W. Washington, DC 20375-5000		PROGRAM ELEMENT NO. 68-7147-91	PROJECT NO.	TASK NO.
		WORK UNIT ACCESSION NO.		
11. TITLE (Include Security Classification) Synthesis and Properties of Mismatched Heterojunction/Substrate Interfaces				
12. PERSONAL AUTHOR(S) Wieder, Harry H.				
13a. TYPE OF REPORT Annual	13b. TIME COVERED FROM 91 Aug 27 TO 92 Aug 1	14. DATE OF REPORT (Year, Month, Day) August 1, 1992	15. PAGE COUNT	
16. SUPPLEMENTARY NOTATION				
17. COSATI CODES			18. SUBJECT TERMS (Continue on reverse if necessary and identify by block number)	
FIELD	GROUP	SUB-GROUP		
19. ABSTRACT (Continue on reverse if necessary and identify by block number)				
<p>Unstrained $\text{In}_x\text{Ga}_{1-x}\text{As}$ and $\text{In}_y\text{Al}_{1-y}\text{As}$ layers and heterostructures lattice matched to each other but mismatched with respect to their GaAs substrates were grown by molecular beam epitaxy using compositionally step graded buffer layers to relax the mismatch strain by more than 90% and their structure, composition, electrical and optical properties were investigated. For $x = 0.3$ the buffer layer is stabilized by dislocation loops. Two-dimensional electron gas in modulation doped heterostructures exhibit a 300 K mobility rising from $9 \times 10^3 \text{ cm}^2/\text{V-s}$ for $x = 0.3$ to $1.1 \times 10^4 \text{ cm}^2/\text{V-s}$ for $x = 0.45$ and an estimated conduction band offset, $\Delta E_c \sim 0.67$ times the bandgap difference between the quantum well and the barrier layer.</p>				
20. DISTRIBUTION/AVAILABILITY OF ABSTRACT <input checked="" type="checkbox"/> UNCLASSIFIED/UNLIMITED <input type="checkbox"/> SAME AS RPT. <input type="checkbox"/> DTIC USERS			21. ABSTRACT SECURITY CLASSIFICATION Unclassified	
22a. NAME OF RESPONSIBLE INDIVIDUAL Dr. Neal Wilsey, Code 6870, NRL			22b. TELEPHONE (Include Area Code) (202) 767-3693	22c. OFFICE SYMBOL

Table of Contents

Abstract	1
Objective	2
Introduction	2
Relaxed buffer layers; methods and procedures	7
Results and Conclusions	8
References	11
Appendix 1	13
Appendix 2	14
Appendix 3	15
Appendix 4	16
Appendix 5	17

92 8 10 122

92-22640



420 900

54Pg

Abstract

Unstrained $\text{In}_x\text{Ga}_{1-x}\text{As}$ and $\text{In}_y\text{Al}_{1-y}\text{As}$ layers and heterostructures lattice matched to each other but mismatched with respect to their GaAs substrates were grown by molecular beam epitaxy using compositionally step graded buffer layers to relax the mismatch strain by more than 90% and their structure, composition, electrical and optical properties were investigated. For $x = 0.3$ the buffer layer is stabilized by dislocation loops. Two-dimensional electron gas in modulation doped heterostructures exhibit a 300 K mobility rising from $9 \times 10^3 \text{ cm}^2/\text{V-s}$ for $x = 0.3$ to $1.1 \times 10^4 \text{ cm}^2/\text{V-s}$ for $x = 0.45$ and an estimated conduction band offset, $\Delta E_c \sim 0.67$ times the bandgap difference between the quantum well and the barrier layer.

DTIC QUALITY INSPECTED 5

Accession For	
NTIS GRA&I	<input checked="checked" type="checkbox"/>
DTIC TAB	<input type="checkbox"/>
Unannounced	<input type="checkbox"/>
Justification	
By	
Distribution/	
Availability Codes	
Dist	Avail and/or Special
A-1	

Objective:

The principal objective of the research performed during the past year concerns the synthesis, growth and evaluation of the properties of arbitrary thickness, unstrained, heterostructures of the ternary alloy system $\text{In}_x\text{Ga}_{1-x}\text{As}/\text{In}_y\text{Al}_{1-y}\text{As}$ whose lattice constants are matched to each other but are mismatched relative to their GaAs substrates. In order to relax the mismatch-induced strain, compositionally step-graded buffer layers are interposed between these heterostructures and their substrates. A further objective of this program is to gradually increase the fractional indium concentration of the strain-relaxed heterostructures up to that of $\text{In}_{0.53}\text{Ga}_{0.47}\text{As}/\text{In}_{0.52}\text{Al}_{0.48}\text{As}$, a heterostructure which is lattice matched to InP. Ultimately, we expect to have an across-the-board comparison of the properties and potential device applications of such strain-relaxed heterostructures grown on GaAs with others grown on InP substrates.

Introduction

In order to grow low defect density, unstrained epitaxial layers on lattice mismatched substrates intermediate buffer layers can be used to contain and to relax the interfacial strains. Strain relaxation between an epilayer and its substrate can proceed by the formation of interfacial dislocations and of threading dislocations which propagate through the epilayer. Partial relaxation of the strain by relatively few threading dislocations can occur if the mismatch is slight. If the layer thickness is less than some specific critical value then the strain can be accommodated by an elastic, essentially tetragonal deformation defined as the pseudomorphic regime.

Relaxed buffer layers investigated thus far fall into several distinct categories: firstly, there are uniform, homogenous thick layers in which the entire change in lattice constant relative to the substrate occurs at the substrate/buffer interface; an example is GaAs grown on silicon which may have $10^{12} / \text{cm}^2$ threading dislocations with the defect densities decreasing over several μm in thickness. A second category is based on the introduction into these thick layers of

superlattices, intended to turn the threading dislocations over into the growth plane converting them into misfit dislocations with densities of $10^6 - 10^8 / \text{cm}^2$. A third category employs buffer layers in which the composition or the lattice constant are graded from the substrate to the epilayer. The profile may be linear, such as achieved in MBE by ramping the effusion cell temperatures or by step grading the buffer layer. For optimizing the relaxation process appropriate choices must be made of the step thickness as well as of the total buffer thickness. An evaluation of strain relaxation requires detailed studies of the correlation between structural characteristics of the epilayers and their synthesis and growth.

For $\text{In}_x\text{Ga}_{1-x}\text{As}$ epilayers grown on GaAs substrates if the mismatch strain is less than 1.25% then the threading dislocation density can be less than $\sim 10^6 / \text{cm}^2$ while for higher strains such as produced by increasing indium concentrations the threading dislocation density may quickly exceed $10^8 / \text{cm}^2$. Buffer structures chosen to offset large mismatches must confine and relax the interfacial strains. Ideally, such buffers must force the threading dislocations to glide to the edges of the heterostructures or pin them within the buffer layers. It has been demonstrated that linearly or step-graded compositional buffer layers can be very effective in performing the function of dislocation barriers^[1-5]. Both, linear or step graded buffer layers require appropriate compositional gradients using, preferably, the minimum number of steps to achieve strain relaxation consistent with thermal and temporal stability of the dislocation network in the buffer layers.

Electrical and structural investigations on partially relaxed $\text{In}_{0.08}\text{Ga}_{0.92}\text{As}/\text{GaAs}$ diodes were made by Choi et al^[6] including double crystal x-ray rocking curve(XRC), optically induced beam currents (OBIC) and optical Nomarski-type topographic investigations. Their XRC data indicates that as the layer thickness increases the lattice relaxation is 4% for a thickness of 0.1 μm , 41% for 0.25 μm and 73% for 1 μm . The average spacing, D, of 60° misfit dislocations is 8.7 μm for 0.1 μm , 89nm for 0.25 μm and 46nm for a thickness of 1 μm . OBIC images showed clearly an increase in crosshatched patterns with increasing thickness suggesting a corresponding increase in misfit dislocations with increasing thickness. Their current vs voltage measurements

showed a deviation from the expected thermionic emission model as the epilayer thickness increased and was attributed, principally, to electron/hole recombination at defects localized within the interfaces. For the 1 μm thick layer they suggest that a Fermi level pinning may occur by a high density of donor-like interfacial traps at $E_v + 0.36\text{eV}$. The average charged interface density, N_s , shows a linear dependence on the in-plane mismatch; it can be represented by $N_s = 2.7\Delta a_{11}/a_0^3$, where a_0 is the mean lattice constant and Δa_{11} is the difference in the parallel lattice constants; a reasonable estimate from their data is $N_s = 4.2 \times 10^{12}/\text{cm}^2$. The interface dislocation structures in $\text{In}_x\text{Ga}_{1-x}\text{As}/\text{GaAs}$ for indium fractions between $x=0.15$ and $x=0.40$ and thicknesses between 60 and 300 nm is complex^[7-9]; the dislocations have one of the four available $(1/2)\langle 110 \rangle$ Burgers vectors oriented 60° to their $\langle 110 \rangle$ direction^[8,9]. Breen et al^[7] found an asymmetric array of linear misfit dislocations parallel to $[011]$ and for $\text{In}_x\text{Ga}_{1-x}\text{As}$ with $x \leq 0.25$; the asymmetry was attributed to different mobilities of α and β dislocations. As the spacing between dislocations decreases and approaches that needed for complete relaxation the asymmetry decreases substantially. For higher x the distribution of the dislocations becomes random, segmented and threading. Partial dislocations and stacking faults were observed frequently for higher x values. As the $\text{In}_{0.25}\text{Ga}_{0.75}\text{As}$ epilayer thickness increases from 20 to 60 nm the average linear dislocation density increases by more than one order of magnitude. However, the measured dislocation densities are inadequate for a complete relaxation of the interfacial strain thus implying a partitioning of the strain between elastic and plastic components.

In 300 nm thick layers dislocation pinning was observed; it is probably responsible for nucleating dislocations in the preliminary stages of strain relaxation and inhibiting their motion in the latter stages of this process.

The threshold for plastic relaxation of an epilayer relative to its substrate has been described in terms of two models. The Matthews and Blakeslee (MB) model^[10] defines a critical thickness in terms of mechanical equilibrium applied to misfit strain which is accommodated by two perpendicular non-interacting arrays of edge dislocations arranged in a square network and

other hand, assumes that interfacial misfit dislocations will be generated if the area strain energy density of the epilayer exceeds the energy density associated with the formation of a dislocation at a distance equal to the layer thickness. Note that MB depends on the propagation of an existing dislocation in the substrate into the epilayer while PB considers the minimum energy required to generate a dislocation (a screw dislocation is considered to have the lowest energy density).

Dixon and Goodhew^[12] found that for strains up to 1.75% two critical thicknesses can be identified: a critical thickness identified with the transformation of threading dislocations into misfit dislocations; this takes place for thicknesses within the range predicted by the MB model while an order of magnitude larger critical thickness, which agrees quite well with the prediction of the PB model, is related to the threshold for nucleation of new dislocations.

The PB model suggests that relaxation at its critical thickness is discontinuous, catastrophic and complete. However, the work of Dunstan et al^[13] indicates that the relaxation is not discontinuous and that the strain during plastic relaxation can be adequately described by a relation of the form $\epsilon = k(b/d)$, where the constant of proportionality, k , is of the order unity; b , is Burger's vector and d is the epilayer thickness. As relaxation proceeds, the stress decreases and when it reaches the elastic limit of the particular $\text{In}_x\text{Ga}_{1-x}\text{As}$ layer further relaxation is impeded leaving a residual strain. Similar considerations were developed theoretically by Hu^[14]. He argues that the misfit dislocations density increases gradually with epitaxial thickness approaching asymptotically the magnitude required for complete relaxation.

The ultimate density of defects in heteroepitaxial layers depends not only on the lattice parameter mismatch but also on the growth mode and on the defect generation mechanism effective during the initial stages of growth. Three different growth modes might be applicable: two-dimensional growth, island growth, and Stranski-Krastanov growth (initial layer growth changing into island growth at a certain layer thickness). Lentzen et al^[15] have investigated the growth mode and strain relaxation during the initial stages of $\text{In}_x\text{Ga}_{1-x}\text{As}$ growth on GaAs (001) substrates. They found that for nominally 5nm thick $\text{In}_x\text{Ga}_{1-x}\text{As}$ the growth is two-dimensional

substrates. They found that for nominally 5nm thick $\text{In}_x\text{Ga}_{1-x}\text{As}$ the growth is two-dimensional and the layers remain pseudomorphic with increasing x up to $x=0.4$ which corresponds to a misfit of 2.8% . For $x = 0.4$ island growth is observed with islands present in different sizes and in different stages of relaxation.

Breen et al^[16] also found a fundamental difference in the strain relief mechanism between (5nm thick) $\text{In}_{0.4}\text{Ga}_{0.6}\text{As}$ epilayers grown on GaAs substrates and layers grown with lower, ($x < 0.25$) indium concentrations. An initial homogenous nucleation of dislocation loops and short irregular segments, progresses into dislocation arrays with an irregular orthogonal morphology as the thicknesses of these layers increases. Dislocation loops are nucleated as the layer grows above critical thickness but island growth inhibits any long range propagation of the dislocations. As the thicknesses of the $\text{In}_{0.4}\text{Ga}_{0.6}\text{As}$ layers increases the loops expand and interact forming a tangled network of dislocation segments consisting of segments with differing Burgers vectors. The interface morphology of strained $\text{In}_{0.5}\text{Ga}_{0.5}\text{As}/\text{GaAs}$ heterostructures grown by means of molecular beam epitaxy was examined by Wang et al^[17] using photoluminescence at 77 K. Transition from 2-dimensional to 3-dimensional growth was found to be strongly temperature dependent and to occur well before the generation of misfit dislocations; it occurs at a critical thickness which is of the order of nine monolayers at 470°C and four monolayers at 540°C. Beam and Kao^[18] who investigated step grading as a means for growing $\text{In}_x\text{Ga}_{1-x}\text{As}/\text{GaAs}$ layers with $x > 0.25$ confirm the transition from 2-D growth to 3-D growth accompanied by indium segregation which may also affect the roughening of the growth interfaces and perhaps a heterogenous activation of additional misfit dislocations. They suggest, tentatively, that linear composition grading may be superior to step grading but admit that for the higher indium concentration ternary alloys factors such as growth rate, growth temperature and composition grading have not been optimized as yet. These introductory notes represent a compendium of information and data obtained from the archival literature relevant to heteroepitaxial growth beyond the pseudomorphic limit of $\text{In}_x\text{Ga}_{1-x}\text{As}/\text{GaAs}$ heterostructures. It set the scene and has affected strongly the methods and procedures of our research described

Relaxed buffer layers; methods and procedures.

At this time, there are no generally applicable design rules or a good theoretical framework for choosing a specific buffer layer which, by the plastic relaxation of mismatch strain will generate dislocations and confine them within the buffer layer. The strain-relaxed buffer should, ideally, provide an effective lattice constant for the heteroepitaxial growth of unstrained, arbitrary thickness, layers or lattice matched heterostructures.

In light of the issues and constraints outlined above our research program was designed to deal with strain-relaxed $\text{In}_x\text{Ga}_{1-x}\text{As}$ layers with $0.25 < x < 0.40$. This is likely to be the transition range from 2-dimensional to 3-dimensional growth. Furthermore, we expected to encounter and to overcome the close correlation between 3-dimensional growth and layer degradation observed by others.

We also expected to test, verify, and, if possible, improve on the empirically developed concepts for strain relaxation by means of buffer layers. We selected for detailed investigations strain-relaxed nominally $\text{In}_{0.3}\text{Ga}_{0.7}\text{As}$ layers grown by MBE on undoped, semi-insulating GaAs substrates covered by an initially grown undoped, thick, GaAs layer on which were deposited, compositionally step-graded nominally $0.3 \mu\text{m}$ thick buffer layers with $\Delta x = 0.1/\text{step}$. These parameters were chosen in order to obtain as nearly as possible 100% strain relaxation within the buffer layers.

The lattice constant of $\text{In}_{0.3}\text{Ga}_{0.7}\text{As}$, assuming Vegard's law to be applicable, is 5.7748 Angstroms. It can be lattice matched by the ternary alloy $\text{In}_{0.29}\text{Al}_{0.71}\text{As}$. Therefore, $\text{In}_{0.3}\text{Ga}_{0.7}\text{As}/\text{In}_{0.29}\text{Al}_{0.71}\text{As}$ lattice matched heterojunctions were deposited on the above described step-graded buffer layers. The $\text{In}_{0.29}\text{Al}_{0.71}\text{As}$ layers doped with silicon provide, by modulation doping, two-dimensional electron gas (2DEG) channels in the $\text{In}_{0.3}\text{Ga}_{0.7}\text{As}$ side of the heterojunctions. Electrical, galvanomagnetic and Shubnikov de Haas measurements of these 2DEG channels can provide information on the nature of the heterojunction interfaces. Also required, particularly for device applications, are correlations derived between the structural characteristics and the corresponding electrical and optical properties of the strain-relaxed

required, particularly for device applications, are correlations derived between the structural characteristics and the corresponding electrical and optical properties of the strain-relaxed epilayers and heterojunctions

Results and Conclusions.

Samples were grown by molecular beam epitaxy on (001)- oriented GaAs substrates cut 2° off towards the [010]-direction. They consist of an initial $0.2 \mu\text{m}$ thick undoped GaAs layer followed by three step-graded layers, each $0.3 \mu\text{m}$ thick, of $\text{In}_x\text{Ga}_{1-x}\text{As}$ with nominal In molar fractions, respectively, of $x=0.1, 0.2$ and 0.3 . Superimposed on this buffer layer is a 10nm thick, undoped $\text{In}_{0.29}\text{Al}_{0.71}\text{As}$ spacer layer, followed by a 30nm thick $\text{In}_{0.29}\text{Al}_{0.71}\text{As}$ Si-doped ($N_d = 1 \times 10^{18}/\text{cm}^3$) layer for modulation doping purposes and topmost is a 10nm thick Si-doped ($N_d = 3 \times 10^{17}/\text{cm}^3$) cap layer. X-ray rocking curves (XRC) were used to determine, in conjunction with plan view and transmission electron microscopy, the structural characteristics of such specimens. We find that the buffer layer produces essentially total relaxation with less than $2 \times 10^6/\text{cm}^2$ dislocations in the $\text{In}_{0.3}\text{Ga}_{0.7}\text{As}$ layer. Further details of this work are provided in the enclosed reprint of our paper by J.C.P Chang et al^[19] which also points out the correlation between the electrical and galvanomagnetic properties of the 2DEG channel in the $\text{In}_{0.3}\text{Ga}_{0.7}\text{As}$ layer which has a sheet electron density of $1.2 \times 10^{12}/\text{cm}^2$ and peak mobilities of $9300 \text{ cm}^2/\text{V}\cdot\text{s}$ at room temperature and $31000 \text{ cm}^2/\text{V}\cdot\text{s}$ at 77 K .

Further details on the properties of the 2DEG in such structures is provided in our paper by Chen et al^[20] appended herewith. Shubnikov de Haas (SdH) oscillatory magnetoresistance measurements made at 1.6 K show that the relaxation time, related to low angle scattering of the 2DEG is $\tau_q = 8.8 \times 10^{-14} \text{ s}$. The effective electron mass at the Fermi level calculated is $m^* = 0.066 m_0$, (where m_0 is the rest mass), is greater by about 20% than that of unstrained $\text{In}_{0.29}\text{Al}_{0.71}\text{As}$ due to the non parabolic correction required for the effective mass of electrons at the Fermi level. On the other hand the classical relaxation time, which depends on the total scattering cross-section is $\tau_c = 1.5 \times 10^{-12} \text{ s}$. The ratio, $\tau_c/\tau_q = 17$, is comparable to the 2DEG of

high

quality $\text{Al}_x\text{Ga}_{1-x}\text{As}/\text{GaAs}$ heterojunctions.

Subsequent investigations of the structural aspects of such 3- step buffered heterojunctions were reported by Kavanagh et al at the Conference on the Physics and Chemistry of Semiconductor Interfaces, Death Valley CA., Feb, 1992 and will be published^[21] in the Proceedings of the PCSI; a preprint is enclosed herewith. Transmission electron microscopy reveals the presence of dislocation loops at the substrate interface, within the substrate, as well as in the first two layers of the buffer. The top layer of the buffer is devoid of any threading dislocations. XRC measurements show a tilt of $\sim 0.3^\circ/\text{step}$. The tilt axis along is 45° to that of the offset axis along [100]. The tilt axis is parallel to the line direction of the dislocation array producing an anisotropy in density of the orthogonal array of misfit dislocations such that the maximum strain relaxation occurred in the [110]-direction. The dislocations give rise to dislocation scattering. It comes as no surprise, therefore, that we observe a $\sim 4\%$ anisotropy of the electron mobility of the 2DEG; the correlation is clear evidence of the significance of dislocation scattering in the effective mobility of the 2DEG. We find, in agreement with the work of Morris et al^[22] made on thick $\text{In}_x\text{Ga}_{1-x}\text{As}/\text{GaAs}$ heterostructures with $x=0.12$ and $x=0.16$, that the anisotropic properties are induced by nonuniform strain relaxation.

We have not succeeded, as yet, in making a four-step compositionally graded buffer with $\Delta x=0.1/\text{step}$ in order to obtain a topmost strain-relaxed $\text{In}_{0.4}\text{Ga}_{0.6}\text{As}$ layer. Transmission electron microscopy of the buffer indicated a large number of lattice defects and the absence of dislocation loops such as found for the 3-step structures. Instead the dislocation array is irregular and tangled suggesting a three-dimensional growth process such as found by others, described in the introductory section, above. There appears to be a transition region between 2-D and 3-D growth between $x=0.3$ and $x=0.4$. However, this is not an impediment for some 2DEG applications as described in our preliminary work described below

accepted for publication in the Aug. 31, 1992 issue of Applied Physics Letters^[24]. In it we show that the sheet electron density, n_s , and mobility, μ , of the 2DEG of strain relaxed $\text{In}_x\text{Ga}_{1-x}\text{As}/\text{In}_y\text{Al}_{1-y}\text{As}$ lattice matched heterostructures with $x \leq 0.45$, the same $10^{18}/\text{cm}^3$ Si-doping concentration in the barrier layer and the same device configuration exhibits a slight increase in $\mu(x)$ from $9 \times 10^3/\text{cm}^2/\text{V-s}$ for $x=0.07$ to $1.05 \times 10^4/\text{cm}^2/\text{V-s}$ for $x=0.45$. The sheet electron density, n_s , increases monotonically from about $7 \times 10^{11}/\text{cm}^2$ at $x=0.07$ to about $1.3 \times 10^{12}/\text{cm}^2$ at $x=0.4$ and then drops to $1.1 \times 10^{12}/\text{cm}^2$ at $x=0.50$. This is attributed to the conduction band offset, $\Delta E_c \sim 0.67 \Delta E_g$, where ΔE_g is the difference between the fundamental bandgaps of the barrier and quantum well and to the transition from the direct to the indirect bandgap of $\text{In}_y\text{Al}_{1-y}\text{As}$ for $y > 0.3$. We find a maximum in $\Delta E_c = 0.72 E_g$ at $x=0.3$ and $y=0.29$. In contrast to the near-independence of μ on the In concentration at room temperature we find a monotonic decrease at 77 K from $\mu = 6 \times 10^4/\text{cm}^2/\text{V-s}$ for $x=0.07$, to a broad minimum near $x=0.4$ of $\mu = 3.2 \times 10^4/\text{cm}^2/\text{V-s}$, attributed, principally, to a combination of alloy scattering and remote impurity scattering.

In conclusion, the work performed during the past year demonstrates a close correlation between the structural, electrical and the galvanomagnetic properties of the strain-relaxed, lattice matched heterojunctions $\text{In}_x\text{Ga}_{1-x}\text{As}/\text{In}_y\text{Ga}_{1-y}\text{As}$ with $x=0.3$ grown on a compositionally step-graded buffer on GaAs substrates. It illustrates potentially important device applications of the two-dimensional electron gas produced by modulation doping in the quantum well of the lower bandgap material and suggests other beneficial electronic and electro-optic applications to be developed in the course of this research program.

References

1. M.S. Abrahams, L.R. Weisberg, C.J. Buiocchi and J. Blank, *J. Mat. Sci.* 4, 223 (1969)
2. G.H. Olsen, M.S. Abrahams, C.J. Buiocchi and T.J. Zamerowski, *J. Appl. Phys.* 46, 1643 (1975)
3. E.A. Fitzgerald, Y-h. Xie, M.L. Green, D. Brasen, A.R. Kortan, J. Michel, Y-J. Mii and B. E. Weir, *Appl. Phys. Lett.* 59, 811 (1991)
4. K. Chang, P. Bhattacharya and R. Lai, *J. Appl. Phys.* 3323 (1990)
5. K. Inoue, J.C. Harmand and T. Matsuno, *J. Cryst. Growth*, 111, 313 (1991)
6. Y.W. Choi, C.R. Wie, K.R. Evans and C.E. Stutz, *J. Appl. Phys.* 68, 1303 (1990)
7. K.R. Breen, P.N. Uppal and J.S. Ahearn, *B7*, 758 (1989)
8. K. Rajan, R. Devine, W.T. Moore and P. Maigne, *J. Appl. Phys.* 62, 1713 (1987)
9. C. Herbaux, J. Di Persio and A. Lefebvre, *Appl. Phys. Lett.* 54, 1005 (1989)
10. J.W. Matthews and A.E. Blakeslee, *J. Cryst. Growth*, 27, 118 (1974)
11. R. People and J.C. Bean, *Appl. Phys. Lett.* 47, 322 (1985)
12. R.H. Dixon and P.J. Goodhew, *J. Appl. Phys.* 68, 3163 (1990)
13. D.J. Dunstan, P. Kidd, L.K. Howard and R.H. Dixon, *Appl. Phys. Lett.* 59, 3390, (1991)
14. S.M. Hu, *J. Appl. Phys.* 69, 7901 (1991)
15. M. Lentzen, D. Gerthsen, A. Forster and K. Urban, *Appl. Phys. Lett.* 60, 74 (1992)
16. K.R. Breen, P.N. Uppal and J.S. Ahearn, *J. Vac. Sci. Technol. B8*, 730 (1990)
17. S.M. Wang, T.G. Andersson and M.J. Ekensedt, *Appl. Phys. Lett.* 59, 2156 (1991)
18. E.A. Beam III and Y. C. Kao, *J. Appl. Phys.* 69, 4253 (1991)
19. J.C.P. Chang, J. Chen, J.M. Fernandez, H.H. Wieder and K.L. Kavanagh, *Appl. Phys. Lett.* 60, 1129 (1992)

20. Jianhui Chen, J.M. Fernandez, J.C.P. Chang, K.L. Kavanagh and H.H. Wieder, *Semicond. Sci. Technol.* 7, 601 (1992)
21. K.L. Kavanagh, J.C.P. Chang, J. Chen, J.M. Fernandez and H.H. Wieder, *J. Vac. Sci. Technol.* July/August (1992), accepted for publication.
22. D. Morris, Q. Sun, C. Lacelle, A.P. Roth, J.L. Brebner, M. Simard-Normandin and K. Rajan, *J. Appl. Phys.* 71, 2321 (1992)
23. Jianhui Chen, J.M. Fernandez and H.H. Wieder, accepted for publication *Proceedings of the 1992 Spring, San Francisco Symp. Mat. Res. Society*
24. Jianhui Chen, J.M. Fernandez and H.H. Wieder, accepted for publication. *Appl. Phys. Lett.* 61 (1992)

Strain relaxation of compositionally graded $\text{In}_x\text{Ga}_{1-x}\text{As}$ buffer layers for modulation-doped $\text{In}_{0.3}\text{Ga}_{0.7}\text{As}/\text{In}_{0.29}\text{Al}_{0.71}\text{As}$ heterostructures

J. C. P. Chang, Jianhui Chen, J. M. Fernandez, H. H. Wieder, and K. L. Kavanagh
Department of Electrical and Computer Engineering, 0407, University of California, San Diego, La Jolla, California 92093-0407

(Received 3 October 1991; accepted for publication 12 December 1991)

Modulation-doped $\text{In}_{0.3}\text{Ga}_{0.7}\text{As}/\text{In}_{0.29}\text{Al}_{0.71}\text{As}$ heterostructures have been grown on GaAs substrates by molecular beam epitaxy using a compositionally step-graded $\text{In}_x\text{Ga}_{1-x}\text{As}$ buffer layer. We found that the buffer layer produces essentially total relaxation with $<2 \times 10^6/\text{cm}^2$ dislocations present in the $\text{In}_{0.3}\text{Ga}_{0.7}\text{As}$ layer. The structural perfection of this layer is reflected in the electrical and galvanomagnetic properties of its two-dimensional electron-gas channel which has a sheet-electron density of $1.2 \times 10^{12}/\text{cm}^2$, peak mobilities of $9\,300\text{ cm}^2/\text{Vs}$ at room temperature and $31\,000\text{ cm}^2/\text{Vs}$ at 77 K, and a mobility anisotropy of $\sim 4\%$ along orthogonal $\langle 110 \rangle$ directions.

Modulation-doped $\text{In}_x\text{Ga}_{1-x}\text{As}/\text{In}_y\text{Al}_{1-y}\text{As}$ heterostructures lattice mismatched to GaAs are important for device applications, including heterojunction-bipolar transistors and modulation-doped field-effect transistors. However, such applications are limited in composition and thickness due to strain relaxation and the formation of lattice defects induced by the lattice mismatch between interfaces.¹ In general, the approach to growing highly lattice-mismatched epilayers is to interpose a buffer layer between the substrate and the active layers. The ideal buffer layer must be fully relaxed yet prevent dislocations from propagating into the active layers. For this purpose, linearly graded,²⁻⁵ step-graded,⁶ superlattice,^{7,8} and combinations of superlattice and step-graded buffer layers⁹ have been used for the lattice-mismatched system.

In this paper, we present strain-relaxation studies of compositionally step-graded $\text{In}_x\text{Ga}_{1-x}\text{As}$ buffer layers using x-ray rocking curves in conjunction with plan-view and cross-sectional transmission electron microscopy (TEM). We relate the structural data to the electrical properties of a superimposed heterojunction containing a two-dimensional electron-gas (2DEG) channel produced by modulation doping.

Samples were grown¹⁰ by molecular beam epitaxy, on (001)-oriented GaAs substrates cut 2° off towards the [010] direction. The grown structure consists of an initial $0.2\text{-}\mu\text{m}$ -thick undoped-GaAs layer, followed by a three-step graded-buffer layer consisting of undoped, $0.3\text{-}\mu\text{m}$ -thick $\text{In}_x\text{Ga}_{1-x}\text{As}$ layers with nominal In molar fractions of $x = 0.1, 0.2$, and 0.3 . Superimposed on this buffer layer is a 10-nm -thick, undoped- $\text{In}_{0.29}\text{Al}_{0.71}\text{As}$ spacer layer, a 30 nm Si-doped ($N_d = 1 \times 10^{18}/\text{cm}^3$) $\text{In}_{0.29}\text{Al}_{0.71}\text{As}$ charge supply layer, and topmost is a 10 nm Si-doped ($N_d = 3 \times 10^{17}/\text{cm}^3$) GaAs cap layer.

To determine the alloy composition and the strain relaxation of the three-step buffer layer, (004) and (224) x-ray rocking curves were measured with a high-resolution x-ray diffractometer using $\text{CuK}\alpha_1$ radiation.¹¹ In general, the peak separation $\Delta\theta$ between an epilayer peak and the substrate peak consists of three components:¹² (1) the difference in the Bragg angle due to the different d spacing, $\Delta\theta_B$, (2) the tilt angle between the epilayer and the sub-

strate reflecting plane (hkl) due to the tetragonal distortion, $\Delta\phi$, and (3) the misorientation angle between the epilayer and the substrate (001) planes, Ω :

$$\Delta\theta = \Delta\theta_B + \Delta\phi \pm \Omega, \quad (1)$$

$$\Delta\theta_B = -\tan\theta_B(\cos^2\phi\epsilon_{001}^x + \sin^2\phi\epsilon_{110}^x \text{ or } \bar{1}\bar{1}0), \quad (2)$$

$$\Delta\phi = \pm \sin\phi \cos\phi(\epsilon_{001}^x - \epsilon_{110}^x \text{ or } \bar{1}\bar{1}0), \quad (3)$$

where θ_B is the Bragg angle of the substrate, ϕ is the angle between the surface and the reflecting planes, and ϵ_{001}^x , ϵ_{110}^x , and $\epsilon_{\bar{1}\bar{1}0}^x$ are x-ray strains in the layer measured with respect to the substrate for the [001] and the two [110] in-plane directions, respectively.

ϵ_{001}^x and the misorientation angle Ω were determined from symmetric (004) rocking curves, where $\Delta\phi = 0$.¹²⁻¹⁵ Rocking curves from (004) reflections were taken for eight azimuthal angles in 45° increments from $\omega = 0^\circ$ – 315° . The azimuthal orientation ω of the sample is defined as a clockwise rotation around the [001] axis; at $\omega = 0^\circ$ the projections of the incident and the diffracted beam lie along the [110] direction. Figure 1 shows four of the eight (004) rocking curves taken for azimuthal angles in 90° increments from $\omega = 0^\circ$ – 270° . For $\omega = 0^\circ$, three peaks corresponding to each layer were well resolved (peak width ~ 1100 arcsec), while, for $\omega = 180^\circ$, the peaks overlapped. This result is due to the fact that the misorientation Ω for each layer with respect to the substrate was different and comparable to the differences in the layer Bragg angles. The variation of the $\text{In}_{0.3}\text{Ga}_{0.7}\text{As}$ -GaAs peak separation $\Delta\theta(004)$ with azimuthal angle ω was fit by the sinusoid^{16,17} $\Delta\theta(004) = -[3217 + 3076 \cos(\omega - 0^\circ)]$ arcsec. Thus the (001) axis of the top buffer layer was tilted with respect to that of the GaAs substrate by 3076 arcsec or 0.854° towards the [110] direction. The average peak separation, -3217 arcsec, was then used to determine ϵ_{001}^x , 2.4% . A similar sinusoidal relationship showed that the $\text{In}_{0.2}\text{Ga}_{0.8}\text{As}$ peak was tilted by 1946 arcsec or 0.55° from the substrate towards the [110] direction. Both tilts are towards a direction 45° to the offcut direction.

A large tilt in an epilayer after a large strain relaxation is a known phenomenon.¹⁸ For example, Wie *et al.* re-

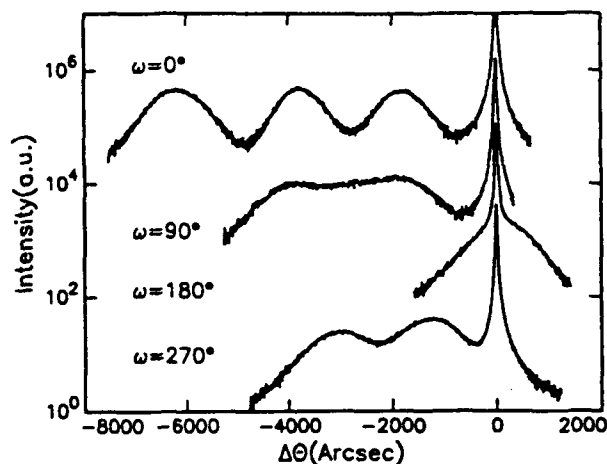


FIG. 1. (004) x-ray rocking curves of a three-step, compositionally graded, $\text{In}_x\text{Ga}_{1-x}\text{As}$ buffer layer ($x = 0.1, 0.2$, and 0.3) taken for four azimuthal angles in 90° increments from $\omega = 0^\circ$ to 270° .

ported a misorientation of 0.35° for a graded $4.5\text{-}\mu\text{m}$ -thick $\text{In}_x\text{Ga}_{1-x}\text{As}$ layer ($x = 0$ to 0.13).¹² In our experience, 0.85° is the largest tilt angle we have encountered and presumably is an indication that this phenomenon scales with the total strain relieved. The tilt and its $[110]$ direction in our case is an indication that the average burgers vector of the interfacial dislocation along the $[110]$ direction has a component perpendicular to the interfaces. We do not yet understand why this imbalance develops.

Knowing ϵ_{001}^x and Ω , ϵ_{110}^x and $\epsilon_{\bar{1}\bar{1}0}^x$ were then determined from four (224) rocking curves (90° apart).¹²⁻¹⁵ The in-plane x-ray strains of the $\text{In}_{0.3}\text{Ga}_{0.7}\text{As}$ layer were then calculated to be $\epsilon_{110}^x = 2.2\%$ and $\epsilon_{\bar{1}\bar{1}0}^x = 1.9\%$. Thus, there is a small asymmetry ($\sim 7\%$) in tetragonal strain relaxation in the two perpendicular $[110]$ directions. The misfit, defined as $\epsilon_f = (a_f - a_s)/a_s$, where a_f is the cubic-cell lattice constant for the completely relaxed film, was calculated from $\epsilon_f = [C_{12}(\epsilon_{110}^x + \epsilon_{\bar{1}\bar{1}0}^x) + C_{11}\epsilon_{001}^x]/(2C_{11} + C_{12})$, where C_{11} and C_{12} are the elastic constants.¹³ The data gives a misfit $\epsilon_f = 2.23\%$ and therefore, the alloy composition $x = 0.31 \pm 0.01$ using Vegard's law. Now, the percentage strain relaxation R ,¹³ defined as $(\epsilon_{110}^x \text{ or } \epsilon_{\bar{1}\bar{1}0}^x / \epsilon_f) 100\%$, and the residual strain ϵ_{\parallel}^r , defined as $(a_{110} \text{ or } a_{\bar{1}\bar{1}0} - a_f/a_f)$ can be calculated. In the top buffer layer the 2.23% strain with respect to the substrate is 98% and 85% relaxed in the two perpendicular in-plane $\langle 110 \rangle$ directions, leaving residual strains of -0.04% and -0.33% , respectively.

A cross-sectional TEM micrograph is shown in Fig. 2. Dislocation loops are frequently seen inside the substrate, the $\text{In}_{0.1}\text{Ga}_{0.9}\text{As}$ layer, and the $\text{In}_{0.2}\text{Ga}_{0.8}\text{As}$ layer, but not in the top $\text{In}_{0.3}\text{Ga}_{0.7}\text{As}$ layer. This is consistent with earlier work on single heterojunctions.^{8,19} No dislocations were observed to thread into the InAlAs layer within the sampling length of the TEM cross-section specimen, $74\text{ }\mu\text{m}$. Thus, this gives an upper limit to the threading dislocation density of $2 \times 10^6/\text{cm}^2$. The step-graded buffer layer effectively relaxed its strain without significant pileup or multiplication of threading dislocations within the $\text{In}_{0.3}\text{Ga}_{0.7}\text{As}$

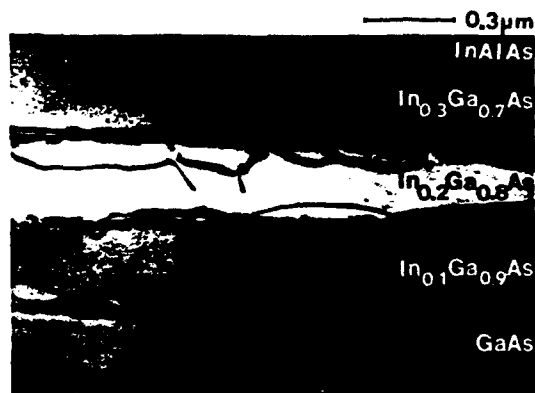


FIG. 2. Cross-sectional transmission electron micrograph of a three-step compositionally graded $\text{In}_x\text{Ga}_{1-x}\text{As}$ buffer layer grown on GaAs.

layer. The second layer, $\text{In}_{0.2}\text{Ga}_{0.8}\text{As}$, has a lighter contrast than the other layers and the substrate, indicating a tilt relative to the other layers, consistent with the x-ray data.

To obtain better statistics for the dislocation density at the $\text{In}_{0.3}\text{Ga}_{0.7}\text{As}/\text{In}_{0.2}\text{Ga}_{0.8}\text{As}$ interface, planar TEM specimens were prepared by chemical thinning from the backside of the substrate until perforation. The specimens are wedge shaped, which means that dislocation densities in the near-surface regions of the sample could be investigated. Figure 3 shows a plan-view TEM micrograph of an area near the hole. The orthogonal dislocation network corresponds to the $\text{In}_{0.2}\text{Ga}_{0.8}\text{As}/\text{In}_{0.3}\text{Ga}_{0.7}\text{As}$ buffer-layer interface. The dislocation density is 2.0×10^5 and $1.6 \times 10^5/\text{cm}$ in the two perpendicular $[110]$ directions. Assuming 60° dislocations, these densities correspond to a lattice relaxation due to dislocations (δ) of 0.4% and 0.32% . Given that the misfit (ϵ_f) between fully relaxed $\text{In}_{0.2}\text{Ga}_{0.8}\text{As}$ and $\text{In}_{0.3}\text{Ga}_{0.7}\text{As}$ layers is 0.7% , the residual strain in the top buffer layer, with respect to the second layer, $\epsilon_{\parallel}^r = \epsilon_f - \delta$, is -0.3% and -0.38% . This is to be

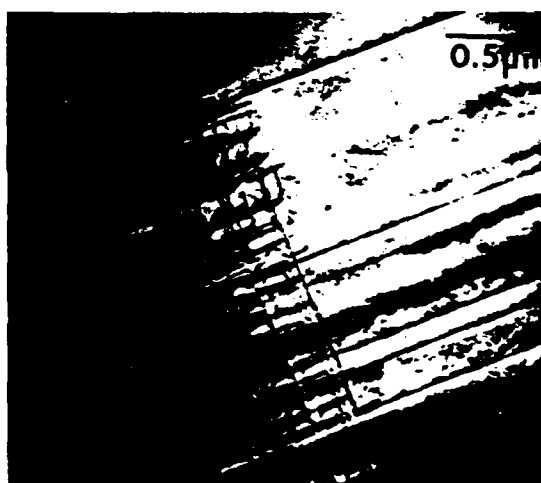


FIG. 3. Plan-view transmission electron micrograph of a three-step, compositionally graded, $\text{In}_x\text{Ga}_{1-x}\text{As}$ buffer layer ($x = 0.1, 0.2$, and 0.3). The orthogonal dislocation network corresponds to the $\text{In}_{0.2}\text{Ga}_{0.8}\text{As}/\text{In}_{0.3}\text{Ga}_{0.7}\text{As}$ buffer-layer interface and the straight dislocations are located at the $\text{In}_{0.3}\text{Ga}_{0.7}\text{As}/\text{In}_{0.2}\text{Ga}_{0.8}\text{As}$ interface.

compared with the x-ray data which measured -0.04% and -0.33% . This difference in one direction may be due to a larger dislocation-density asymmetry at either the substrate/ $\text{In}_{0.1}\text{Ga}_{0.9}\text{As}$ or the $\text{In}_{0.2}\text{Ga}_{0.8}\text{As}/\text{In}_{0.3}\text{Ga}_{0.7}\text{As}$ interface or of course due to the formation of edge-misfit dislocations. The straight dislocations terminate $1\text{ }\mu\text{m}$ distance from the hole and are therefore located at the $\text{In}_{0.3}\text{Ga}_{0.7}\text{As}/\text{In}_{0.29}\text{Al}_{0.71}\text{As}$ interface. They lie along only one $\langle 110 \rangle$ direction and their density, $1 \times 10^4/\text{cm}$, corresponds to a strain relaxation of 0.02% . This is small compared to the actual misfit (0.45%) between $\text{In}_{0.29}\text{Al}_{0.71}\text{As}$ and the 91% on average relaxed $\text{In}_{0.3}\text{Ga}_{0.7}\text{As}$. Thus, the $\text{In}_{0.29}\text{Al}_{0.71}\text{As}$ layer is still predominantly tetragonally distorted. No dislocations were observed in the region right next to the hole associated with the channel within the sampling area of the planar TEM specimen, $135\text{ }\mu\text{m}^2$. This gives us an upper limit to the threading dislocation density of $7 \times 10^5/\text{cm}^2$, consistent with the cross-sectional micrograph.

We have obtained further confirmation of the essentially unstrained character of the $\text{In}_{0.3}\text{Ga}_{0.7}\text{As}$ layer by etching off the topmost InAlAs and GaAs layers from a similar step-graded wafer and measuring the photoluminescence response at 10 K as a function of the wavelength. The peak response at $\lambda = 11\,275\text{ }\text{\AA}$ (1.1 eV and 34 FWHM) is considered to be the fundamental band gap; it is in good agreement with 1.09 eV , that of bulk, unstrained $\text{In}_{0.3}\text{Ga}_{0.7}\text{As}$.

Assuming the 77 K mobility to be limited principally by remote-impurity scattering, alloy scattering, and polar optical-phonon scattering, the estimated mobility² of the two-dimensional electron-gas channel, in the unstrained $\text{In}_{0.3}\text{Ga}_{0.7}\text{As}$ is $\mu \sim 4 \times 10^4\text{ cm}^2/\text{V s}$. Our experimental measurements indicate a small but definite mobility anisotropy along the two orthogonal $\langle 110 \rangle$ directions of about 4% , $\mu = 3.1 \times 10^4\text{ cm}^2/\text{V s}$ and $\mu = 2.96 \times 10^4\text{ cm}^2/\text{V s}$, with corresponding room-temperature mobilities, $\mu = 9340\text{ cm}^2/\text{V s}$ and $\mu = 8990\text{ cm}^2/\text{V s}$. The lower mobility and the mobility anisotropy is attributed to the $\sim 7\%$ anisotropy in strain relaxation and to the asymmetric misfit-dislocation density which adds a dislocation-scattering component to the mobility-limiting mechanism.

We correlate strain relaxation in a compositionally

step-graded $\text{In}_x\text{Ga}_{1-x}\text{As}$ buffer layer to the electrical properties of a modulation-doped $\text{In}_{0.3}\text{Ga}_{0.7}\text{As}/\text{In}_{0.29}\text{Al}_{0.71}\text{As}$ heterostructure grown upon it. X-ray data showed that the 2.23% misfit of the buffer layer was 91% relaxed with a 7% asymmetry in the two $\langle 110 \rangle$ in-plane interface directions. The top $\text{In}_{0.3}\text{Ga}_{0.7}\text{As}$ buffer layer was tilted by 0.85° from the substrate. Plan-view and cross-sectional TEM support the x-ray results. Less than $2 \times 10^6/\text{cm}^2$ dislocations penetrate through the 2DEG channel, which has a sheet-electron density of $1.2 \times 10^{12}/\text{cm}^2$, peak mobilities of $9300\text{ cm}^2/\text{V s}$ at room temperature and $31\,000\text{ cm}^2/\text{V s}$ at 77 K , and a mobility anisotropy of $\sim 4\%$.

This work was supported in part by NSF and the Naval Research Laboratory (N. Wilsey).

- ¹V. Krishnamoorthy, P. Ribas, and R. M. Park, *Appl. Phys. Lett.* **58**, 2000 (1991).
- ²K. Inoue, J. C. Harmond, and T. Matsuno, *J. Cryst. Growth* **11**, 313 (1991).
- ³J. C. Harmond, T. Matsuno, and K. Inoue, *Jpn. J. Appl. Phys.* **29**, L233 (1990).
- ⁴F. K. Legoues, B. S. Meyerson, and J. F. Morar, *Phys. Rev. Lett.* **66**, 2903 (1991).
- ⁵E. A. Fitzgerald, Y.-H. Xie, M. L. Green, D. Brasen, A. R. Kortan, J. Michel, Y.-J. Mii, and B. E. Weir, *Appl. Phys. Lett.* **59**, 811 (1991).
- ⁶K. Chang, P. Bhattacharya, and R. Lai, *J. Appl. Phys.* **67**, 3323 (1990).
- ⁷T. Won, S. Agarwala, and H. Morkoc, *Appl. Phys. Lett.* **53**, 2311 (1988).
- ⁸C. Herbeaux, J. Di Persio, and A. Lefebvre, *Appl. Phys. Lett.* **54**, 1004 (1989).
- ⁹P. Ribas, V. Krishnamoorthy, and R. M. Park, *Appl. Phys. Lett.* **57**, 1040 (1990).
- ¹⁰Jianhui Chen, J. M. Fernandez, J. C. P. Chang, K. L. Kavanagh, and H. H. Wieder (unpublished).
- ¹¹J. C. P. Chang, T. P. Chin, K. L. Kavanagh, and C. W. Tu, *Appl. Phys. Lett.* **58**, 1530 (1991).
- ¹²C. R. Wie, H. M. Kim, and K. M. Lau, *SPIE Proc.* **877**, 41 (1988).
- ¹³C. R. Wie, *J. Appl. Phys.* **65**, 2267 (1989).
- ¹⁴A. Segmuller and M. Murakami, in *Treatise on Materials Science and Technology*, edited by K. N. Tu and R. Rosenberg (Academic, New York, 1988), Vol. 27, pp. 188-200.
- ¹⁵J. Matsui, K. Onabe, T. Kamejima, and I. Hayashi, *J. Electrochem. Soc.* **126**, 664 (1979).
- ¹⁶S. K. Ghandhi and J. E. Ayers, *Appl. Phys. Lett.* **53**, 1204 (1988).
- ¹⁷A. Leiberich and J. Levkoff, *J. Cryst. Growth* **100**, 330 (1990).
- ¹⁸J. E. Ayers, S. K. Ghandhi, and L. J. Schowalter, *J. Cryst. Growth* **113**, 430 (1991).
- ¹⁹K. L. Kavanagh, M. A. Capano, L. W. Hobbs, J. C. Barbour, P. M. J. Maree, W. Schaff, J. W. Mayer, D. Pettit, J. M. Woodall, J. A. Strosio, and R. M. Feenstra, *J. Appl. Phys.* **64**, 4843 (1988).

APPENDIX 2

LETTER TO THE EDITOR

Modulation-doped

$\text{In}_{0.3}\text{Ga}_{0.7}\text{As}/\text{In}_{0.29}\text{Al}_{0.71}\text{As}$ heterostructures grown on GaAs by step grading

Jianhui Chen, J M Fernández, J C P Chang, K L Kavanagh and H H Wieder

Electrical and Computer Engineering Department, 0407, University of California, San Diego, La Jolla, CA 92093-0407, USA

Received 21 January 1992, accepted for publication 6 February 1992

Abstract. Modulation-doped $\text{In}_{0.3}\text{Ga}_{0.7}\text{As}/\text{In}_{0.29}\text{Al}_{0.71}\text{As}$ heteroepitaxial layers were grown on GaAs substrates by molecular beam epitaxy using compositionally graded buffer step layers. The misfit strain in the $x = 0.3$ layer, which contains the two-dimensional electron gas channel, is relaxed by 96% as determined by x-ray diffraction. Transmission electron microscopy reveals that the active layer is dislocation-free. The sheet electron density of the channel is of the order 10^{12} cm^{-2} and the mobility is $9340 \text{ cm}^2 \text{ V}^{-1} \text{ s}^{-1}$ at room temperature and $42290 \text{ cm}^2 \text{ V}^{-1} \text{ s}^{-1}$ at cryogenic temperatures. The effective mass of the electrons, $m^* = 0.066m_0$, is greater by about 20% than that expected of this ternary alloy, due principally to the non-parabolic correction at the Fermi level. Shubnikov-de Haas oscillations measured at 1.6 K as a function of magnetic field show that the quantum relaxation time is $8.8 \times 10^{-14} \text{ s}$ while the classical relaxation time determined from the measured mobility and calculated m^* is $1.5 \times 10^{-12} \text{ s}$.

The ternary alloy system $\text{In}_x\text{Ga}_{1-x}\text{As}$ provides major advantages for electronic and electro-optic device applications because its conduction band offset, relative to GaAs, increases and its effective electron mass, m^* , decreases with increasing indium fraction, x . These advantages are offset, however, by the composition-dependent alloy scattering and by strain, which can produce either elastic or plastic deformation in epitaxially grown $\text{In}_x\text{Ga}_{1-x}\text{As}$ quantum wells (QW) deposited on GaAs substrates.

Tetragonally strained, pseudomorphic QW are used, to advantage, for making high performance field-effect transistors and quantum-confined Stark effect modulators. The onset of plastic deformation and/or the attendant nucleation and propagation of interfacial dislocations limits the practical use of such epilayers to comparatively low indium concentrations, $x \leq 0.2$.

In order to increase the indium concentration and/or the thickness of an epilayer beyond its pseudomorphic limit, a buffer layer can be interposed between it and the GaAs substrate. The composition and structure of this layer are to be chosen such that strain relaxation occurs entirely within the buffer layer without the nucleation of dislocations in the epilayer. For this purpose, linear

compositional grading, step grading, superlattice and combinations of superlattice and step-graded buffer layers have been used [1-9]. Linear graded buffer layers appear to be a particularly effective approach in both SiGe [10, 11] and III-V systems [5, 12].

We have chosen to investigate the synthesis of (as nearly as possible) strain-free $\text{In}_{0.3}\text{Ga}_{0.7}\text{As}$ epilayers grown on GaAs substrates with an intermediate three-step graded buffer layer and to establish, if possible, a quantitative correlation between strain relaxation in the buffer layers and the electrical and the galvanomagnetic properties of the epilayers.

Specimens were grown by molecular beam epitaxy, on (100)-oriented GaAs substrates cut 2° off towards the [110] direction, in a Varian GenII reactor. High energy electron diffraction was used to monitor the growth parameters; As₄/III beam flux ratio of ~ 20 and growth rates of about $1 \mu\text{m h}^{-1}$ were obtained for a substrate temperature kept constant at 535°C .

Structures such as that shown schematically in figure 1 were used for the subsequently described experimental investigations. They consist of an initial $0.2 \mu\text{m}$ thick undoped GaAs layer deposited on the semi-insulating substrate, upon which are grown, sequentially, three

10 nm n-GaAs ($n = 3 \times 10^{17} \text{ cm}^{-2}$)
30 nm n- $\text{In}_{0.29}\text{Al}_{0.71}\text{As}$ ($n = 1 \times 10^{18} \text{ cm}^{-2}$)
10 nm undoped $\text{In}_{0.29}\text{Al}_{0.71}\text{As}$
0.30 μm undoped $\text{In}_{0.30}\text{Ga}_{0.70}\text{As}$
0.30 μm undoped $\text{In}_{0.20}\text{Ga}_{0.80}\text{As}$
0.30 μm undoped $\text{In}_{0.10}\text{Ga}_{0.90}\text{As}$
Semi-insulating GaAs substrate

Figure 1. Schematic cross section of the buffer layer and modulation-doped heterostructure intended to provide a strain-free two-dimensional electron gas channel in a $\text{In}_{0.3}\text{Ga}_{0.7}\text{As}$ layer.

undoped, 0.3 μm thick $\text{In}_x\text{Ga}_{1-x}\text{As}$ layers with In molar fractions, respectively, of $x = 0.1, 0.2$ and 0.3 . The uppermost $\text{In}_{0.3}\text{Ga}_{0.7}\text{As}$ layer contains the two-dimensional electron gas (2DEG) channel induced in it by modulation doping from the superposed 30 nm thick Si-doped ($N_D = 1 \times 10^{18} \text{ cm}^{-3}$) $\text{In}_{0.29}\text{Al}_{0.71}\text{As}$ barrier layer and separated from the 2DEG channel by an undoped, 10 nm thick spacer layer of the same composition as that of the barrier layer. A 10 nm thick GaAs layer doped with Si, $N_D = 3 \times 10^{17} \text{ cm}^{-3}$, is used as a cap layer.

Double-crystal x-ray diffraction was used to determine the strain relaxation of the specimens [13]. The x-ray diffraction peaks of the layers from (400) and (422) reflections were well resolved, leading to the determination of the perpendicular and parallel lattice constants, a_p and $a_{||}$ for each layer. From these data the composition and natural unstrained lattice constant of each layer, a_0 , were calculated. The resulting residual strain $\epsilon_{||} = (a_{||} - a_0)/a_0$, for the $x = 0.3$ layer in the $\langle 100 \rangle$ in-plane directions was -0.085% . Thus, from these data 96% of the strain expected for an $\text{In}_{0.3}\text{Ga}_{0.7}\text{As}/\text{GaAs}$ layer, and consequently present in the 2DEG channel, was relieved by the buffer layer. Cross-section transmission electron microscopy [13] of the structure in figure 1 showed that dislocations are confined at the three step-graded interfaces. In addition, many dislocations were seen to loop into the $\text{In}_{0.1}\text{Ga}_{0.9}\text{As}$ and $\text{In}_{0.2}\text{Ga}_{0.8}\text{As}$ layers. The conduction channel at the $\text{In}_{0.3}\text{Ga}_{0.7}\text{As}/\text{In}_{0.29}\text{Al}_{0.71}\text{As}$ interface is essentially dislocation-free.

The grown layers were processed by means of photolithographic and etching procedures into conventional six-arm Hall bridge structures. Au/Ge eutectic contacts were deposited in vacuum and alloyed in order to make

ohmic connection to the 2DEG in the $\text{In}_{0.3}\text{Ga}_{0.7}\text{As}$ layers. The room-temperature sheet electron concentration of a representative specimen is $n_s = 1.10 \times 10^{12} \text{ cm}^{-2}$ and its electron mobility, determined from conductivity and low-field Hall measurements, is $\mu = 9190 \text{ cm}^2 \text{ V}^{-1} \text{ s}^{-1}$. The best samples measured, thus far, had $n_s = 1.32 \times 10^{12} \text{ cm}^{-2}$ and $\mu = 9340 \text{ cm}^2 \text{ V}^{-1} \text{ s}^{-1}$. Figure 2 shows the temperature dependence of the electron mobility of three samples from different growth but under similar growth conditions. At 77 K the highest mobility is $\mu = 35020 \text{ cm}^2 \text{ V}^{-1} \text{ s}^{-1}$, reaching $42290 \text{ cm}^2 \text{ V}^{-1} \text{ s}^{-1}$ at 30 K and decreasing slightly at lower temperatures, while the sheet electron concentration remains essentially constant at $n_s = 1.21 \times 10^{12} \text{ cm}^{-2}$ below 77 K. These data are the best results reported so far for this composition, indicating the good quality of the active layers. For comparison, Inoue *et al* [5] reported an electron mobility of $7500 \text{ cm}^2 \text{ V}^{-1} \text{ s}^{-1}$ at room temperature and $2.5 \times 10^4 \text{ cm}^2 \text{ V}^{-1} \text{ s}^{-1}$ at 77 K for an $\text{In}_{0.3}\text{Ga}_{0.7}\text{As}$ epilayer grown on GaAs using a linear compositional grading. Their theoretical calculations assuming a superposition of the relaxation processes attributed to impurity scattering, polar optical mode scattering, deformation potential scattering and piezoelectric scattering, but controlled principally by alloy scattering, lead to an effective 77 K mobility, $\mu = 4 \times 10^4 \text{ cm}^2 \text{ V}^{-1} \text{ s}^{-1}$ for $\text{In}_{0.3}\text{Ga}_{0.7}\text{As}$.

We have measured the magnetic field dependence of the ρ_{xx} and ρ_{xy} components of the conductivity tensor of the 2DEG channel of the high mobility specimen, at 1.6 K, using a superconducting magnet with a peak magnetic field of 8 T. The data in figure 3 show that Shubnikov-de Haas oscillations appear above ~ 2.7 T and well resolved ρ_{xy} plateaus, characteristic of the integral quantum Hall effect, appear above ~ 2.8 T. The Fourier transform spectrum of these SdH oscillations shows a single peak, indicating that only one subband is involved in charge carrier transport and that $n_s = 1.2 \times 10^{12} \text{ cm}^{-2}$, in good agreement with the data obtained from the low-field Hall measurements.

A theoretical analysis shown to predict correctly the low magnetic field amplitudes and phases of the SdH

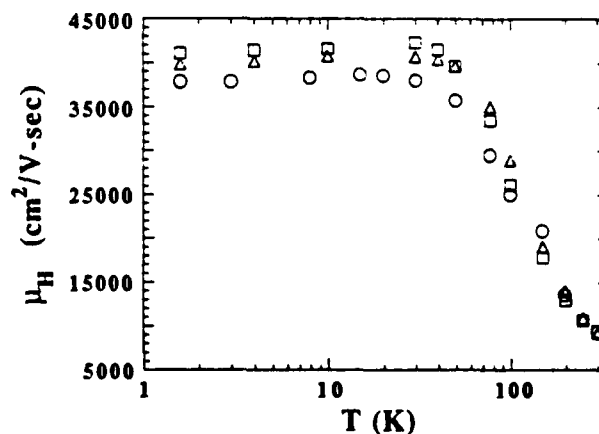


Figure 2. Temperature dependence of the electron mobility of the 2DEG determined from low-field Hall effect and conductivity measurements.

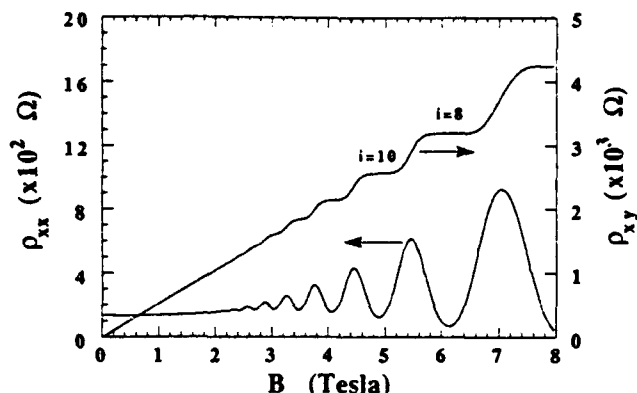


Figure 3. Shubnikov-de Haas magnetoresistance oscillations and integral quantum Hall effect measured at 1.6 K on the $\text{In}_{0.3}\text{Ga}_{0.7}\text{As}$ 2DEG channel. The measuring current was 10 μA and the Landau level index is shown on the ρ_{xy} data.

oscillation was developed by Coleridge *et al* [14]; for the first subband it is

$$\rho_{xx}/\rho_0 = 1 + 4D(X)\exp(-\pi/\omega_c\tau_q)\cos(2\pi E_F/\hbar\omega_c - \pi) \quad (1)$$

where the cyclotron frequency, $\omega_c = qB/m^*$, with B the magnetic field, $X = 2\pi^2 kT/\hbar\omega_c$, $D(X) = X/\sinh X$; E_F is the Fermi energy, k is Boltzmann's constant, T the temperature, \hbar the reduced Planck's constant and τ_q is the quantum relaxation time related to the total scattering rate; it is different from the classical relaxation time τ_c related to the conductivity and the mobility, which is weighted by the scattering angle; large differences have been observed between these relaxation times in modulation-doped III-V heterojunctions, while in silicon MOS structures they are essentially the same.

The effective electron mass in our 2DEG channel is different from that of unstrained $\text{In}_{0.3}\text{Ga}_{0.7}\text{As}$, $m_F^* = 0.055m_0$, due to the non-parabolic correction required for the effective mass at the Fermi level, as shown by Liu *et al* [15] and Ando [16]. Taking the correction into account, we derived $m^*/m_0 = 0.066$, larger by approximately 20% than m_F^*/m_0 . We then used the experimentally determined n_s and the calculated m^* to fit the measured low magnetic field dependent amplitudes of the sdH oscillations, shown in figure 3, by means of equation (1), choosing an appropriate τ_q for this purpose, and from such a simulation we obtain $\tau_q = 8.8 \times 10^{-14}$ s. The classical relaxation time, using the measured 1.6 K mobility $\mu = 41\,050 \text{ cm}^2 \text{ V}^{-1} \text{ s}^{-1}$ and the calculated $m^* = 0.066m_0$ is $\tau_c = 1.5 \times 10^{-12}$ s; therefore $\tau_c/\tau_q = 17$, indicating that total electron scattering is greater by more than one order of magnitude than angle-dependent scattering. The value of this ratio is comparable to results

obtained in high-quality heterojunctions, such as AlGaAs/GaAs [17].

In conclusion, we demonstrate that high-quality $\text{In}_{0.3}\text{Ga}_{0.7}\text{As}/\text{In}_{0.29}\text{Al}_{0.71}\text{As}$ modulation-doped heterostructures can be grown by molecular beam epitaxy on GaAs substrates using compositionally step-graded buffer layers. The growth is repeatable. The room-temperature sheet electron concentration of the two-dimensional electron gas channel located in the $\text{In}_{0.3}\text{Ga}_{0.7}\text{As}$ layer is of the order 10^{12} cm^{-2} , and the high room-temperature mobility and that measured at low temperatures support the view that dislocation scattering is negligible. The calculated effective mass ratio, $m^*/m_0 = 0.066$ is greater than that to be expected for this ternary alloy, $m^*/m_0 = 0.055$. Its larger value is due principally to a non-parabolic correction required for electrons at the Fermi level. Shubnikov-de Haas oscillations as a function of magnetic field show that the quantum relaxation time, $\tau_q = 8.8 \times 10^{-14}$ s, is considerably smaller than the classical relaxation time, $\tau_c = 1.5 \times 10^{-12}$ s, determined from electron mobility measurements.

References

- [1] Won T, Agarwala S and Morkoc H 1988 *Appl. Phys. Lett.* **53** 2311
- [2] Kalem S, Chyi J I, Morkoc H, Bean R and Zanozi K 1988 *Appl. Phys. Lett.* **53** 1647
- [3] Wang G W, Chen Y K, Schaff W J and Eastman L F 1988 *IEEE Trans. Electron Devices* **35** 818
- [4] Harmand J C, Matsuno T and Inoue K 1990 *Japan. J. Appl. Phys.* **29** L233
- [5] Inoue K, Harmand J C and Matsuno T 1991 *J. Cryst. Growth* **111** 313
- [6] Chang K, Bhattacharya P and Lai R 1990 *J. Appl. Phys.* **67** 3323
- [7] Ribas P, Krishnamoorthy V and Park R M 1990 *Appl. Phys. Lett.* **57** 1040
- [8] Fitzgerald E A, Ast D G, Kirchner P D, Pettit G D and Woodall J M 1988 *J. Appl. Phys.* **63** 693
- [9] Krishnamoorthy V, Ribas P and Park R M 1991 *Appl. Phys. Lett.* **58** 2000
- [10] Legoues F K, Meyerson B S and Morar J F 1991 *Phys. Rev. Lett.* **66** 2903
- [11] Fitzgerald E A, Xie Y H, Green M L, Brasen D, Kortan A R, Michel J, Mii Y-J and Weir B E 1991 *Appl. Phys. Lett.* **59** 811
- [12] Kirchner P D 1991 private communication
- [13] Chang J C P, Chen Jianhui, Fernández J M, Wieder H H and Kavanagh K L 1992 *Appl. Phys. Lett.* to be published
- [14] Coleridge P T, Stoner R and Fletcher R 1989 *Phys. Rev. B* **39** 1120
- [15] Liu C T, Lin S Y and Tsui D C 1988 *Appl. Phys. Lett.* **53** 2510
- [16] Ando T 1982 *J. Phys. Soc. Japan* **51** 3893
- [17] Harrang J P, Higgins R J, Goodall R K, Jay P R, Laviron M and Deleschuse P 1985 *Phys. Rev. B* **32** 8126

Final
6/10/92

**Composition dependent transport properties of strain relaxed
 $\text{In}_x\text{Ga}_{1-x}\text{As}$ ($x < 0.45$) epilayers**

Jianhui Chen, J.M. Fernandez, and H.H. Wieder

Department of Electrical and Computer Engineering, 0407,

University of California at San Diego,

La Jolla, CA 92093-0407

Abstract

The concentration and mobility of the two dimensional electron gas present at the interface between strain-relaxed, lattice matched, $\text{In}_y\text{Al}_{1-y}\text{As}/\text{In}_x\text{Ga}_{1-x}\text{As}$ ($x < 0.45$), modulation doped heterojunctions grown by means of compositionally step-graded buffer layers on GaAs substrates, were measured at room temperature and at 77 K. The composition dependence of the electron density is attributed to the dependence of the bandgap energy of $\text{In}_x\text{Ga}_{1-x}\text{As}$ and that of $\text{In}_y\text{Al}_{1-y}\text{As}$ on x , with a conduction band offset, $\Delta E_c \sim 0.67\Delta E_g$. The room temperature electron mobility increases from $9 \times 10^3 \text{ cm}^2/\text{V-s}$ for $x=0.07$ to $1.05 \times 10^4 \text{ cm}^2/\text{V-s}$ for $x=0.45$. Such strain-relaxed heterostructures have higher electron mobilities than similar pseudomorphic structures with the same sheet electron concentration.

PACS numbers: 73.50.-h, 68.55.Bd

Heterojunctions made of the ternary alloy $\text{In}_x\text{Ga}_{1-x}\text{As}$ with other binary or ternary III-V alloys provide a number of advantages for device applications. These include¹ the decrease of the effective electron mass and the increase in the conduction band intervalley energy difference with increasing x . The ternary alloys $\text{In}_{0.53}\text{Ga}_{0.47}\text{As}$ and $\text{In}_{0.52}\text{Al}_{0.48}\text{As}$ have lattice constants which match, exactly, that of InP . Other compositions are either in compressive or tensile strain relative to InP and they are in compressive strain relative to GaAs . Optimum design criteria for many heterostructure devices include the need for a large conduction band offset, ΔE_c , a high electron mobility, μ , and a high saturated velocity, v_s .

For pseudomorphic $\text{In}_x\text{Ga}_{1-x}\text{As}/\text{GaAs}$ heterostructures^{2,3} the difference, ΔE_g , of the fundamental band gaps increases with the fractional indium concentration x , and the conduction band offset, $\Delta E_c \sim Q_c \Delta E_g$ with $Q_c = 0.6$ to 0.7 . The interfacial strain produced by the lattice mismatch, which increases with x , can generate lattice defects unless layer thicknesses are limited below some critical threshold^{4,5} associated with strain relaxation. These defects affect, adversely, the charge carrier transport properties of such heterojunctions.

The large band gaps of $\text{Al}_y\text{Ga}_{1-y}\text{As}$ alloys are useful for modulation doped, pseudomorphic, double heterojunctions of $\text{Al}_y\text{Ga}_{1-y}\text{As}/\text{In}_x\text{Ga}_{1-x}\text{As}/\text{GaAs}$ because^{6,7} $\Delta E_c \sim 0.67 \Delta E_g$ (for $y=0.2$ to 0.35 and $x=0.12$ to 0.35). This provides good confinement of the two-dimensional electron gas (2DEG) in the $\text{In}_x\text{Ga}_{1-x}\text{As}$ quantum wells (QW), a high sheet electron density, n_s , and a low leakage current across the heterojunction interfaces. However, increasing x affects adversely the electron mobility due to the dependence of the electron effective mass,⁸ and other parameters⁹ on strain.

To our knowledge, no detailed theoretical or experimental comparisons have been made, as yet, of pseudomorphic QW heterostructures with similar but strain-relaxed $\text{In}_x\text{Ga}_{1-x}\text{As}$. However, by solving the Boltzmann transport equation

using Monte Carlo techniques, Thobel et al.⁹ have calculated the composition dependence of electron mobility, μ , and of the peak electron velocity, v_s , for bulk, unstrained, and pseudomorphically strained $\text{In}_x\text{Ga}_{1-x}\text{As}$ respectively, grown either on GaAs or on InP substrates. They found that the μ and the v_s are degraded significantly for $\text{In}_x\text{Ga}_{1-x}\text{As}$ layers with $x \geq 0.25$, grown compressively strained on GaAs substrate; but are affected only slightly for $x \geq 0.53$ compressively strained relative to InP. Strain-free heterojunctions may have a higher conduction band offset than their strained counterparts as suggested by the work of Arent et al.¹⁰ and strain-relaxed heterojunctions on GaAs substrate may be useful for device applications which require $E_g > 0.75$ eV. Such heterostructures can be made by interposing a compositionally step graded or a linearly graded buffer layer between them and the GaAs substrate.

In this paper we present experimental results and an interpretation of the composition dependence of n_s and μ of the 2DEG, present in strain-relaxed $\text{In}_x\text{Ga}_{1-x}\text{As}$ layers. These are compared to pseudomorphic $\text{In}_x\text{Ga}_{1-x}\text{As}/\text{Al}_y\text{Ga}_{1-y}\text{As}$ and $\text{In}_x\text{Ga}_{1-x}\text{As}/\text{GaAs}$ heterostructures.

Molecular beam epitaxy was employed to grow the heterostructures on semi-insulating (001)-oriented GaAs substrates with a 2° offcut towards the nearest (110)-plane. A substrate temperature, $T_s = 535^\circ\text{C}$, was used for the growth of $x \leq 0.3$ specimens, otherwise T_s was maintained between 480°C and 510°C . The As_4 equivalent vapor pressure was typically 20 to 30 times that of the group III constituents and the growth rates were between 0.8 and $1.4 \mu\text{m/hr}$. A $0.2 \mu\text{m}$ thick GaAs layer was first grown on the substrate followed by the compositionally graded buffer layers. These consist of $0.3 \mu\text{m}$ thick steps of $\text{In}_x\text{Ga}_{1-x}\text{As}$, with a composition increment, $\Delta x = 0.1/\text{step}$. For modulation doping purposes, a 30 nm thick carrier supply layer doped with Si to nominally $1 \times 10^{18}/\text{cm}^3$ superposed on a 10 nm thick undoped spacer layer, both of lattice matched $\text{In}_y\text{Al}_{1-y}\text{As}$, were subsequently grown

on the appropriate $\text{In}_x\text{Ga}_{1-x}\text{As}$ epilayer. The compositions of the specimens were determined by double crystal x-ray diffraction and, in some instances, the structural properties were studied by transmission electron microscopy.¹¹ Resistivity and Hall effect measurements were made at room temperature and 77 K using a dc current of 10 μA and a magnetic field of 0.1 Tesla on six-arm Hall bar structures processed by means of photolithographic procedures.

Transmission electron microscopy of our specimens, both of cross-section and plan view, show that for $x < 0.3$ the threading dislocation density in the topmost $\text{In}_x\text{Ga}_{1-x}\text{As}$ layer is less than $2 \times 10^6 \text{ cm}^{-2}$. However, asymmetrically distributed misfit dislocations running along mutually orthogonal $\langle 110 \rangle$ directions were observed by TEM. We can expect, therefore, a mobility degradation due to dislocation scattering. It is reflected in the anisotropic electron mobility with maximum μ in the $\langle \bar{1}10 \rangle$ orientation, i.e., with the current density vector oriented along the $\langle \bar{1}10 \rangle$ axis. The subsequently described measurements represent data obtained on specimens with this orientation.

Figure 1 shows the dependence of n_s as a function of x derived from Hall measurements. Because the specimens have the same doping density and geometric parameters, we believe that Fig. 1 represents the composition dependence of the confinement potential of the 2DEG, hence of the conduction band offset, ΔE_c . Explicit measurements of the ΔE_c of such heterostructures have been reported¹² only for $x=0.53$ and $y=0.52$. If $\Delta E_c(x)$ depends principally on the variation of $\Delta E_g(x)$ then one might expect it to increase with x for $x \leq 0.3$ and to decrease for $x > 0.3$. Using the composition dependence¹³ of the fundamental band gap of $\text{In}_x\text{Ga}_{1-x}\text{As}$ and that¹⁴ of the direct band gap ($y > 0.3$) of $\text{In}_y\text{Al}_{1-y}\text{As}$, the band edge differences, ΔE_g , can be expressed for both the direct and the indirect gap by interpolating for the latter ($y < 0.3$) linearly; choosing $y=x-0.01$ for lattice matching $\text{In}_x\text{Ga}_{1-x}\text{As}$ with $\text{In}_y\text{Al}_{1-y}\text{As}$

$$\Delta E_g \text{ (eV)} = 0.738 + 1.161x + 0.436x^2 \quad (\text{for } x < 0.3) \quad (1)$$

$$\Delta E_g \text{ (eV)} = 1.629 - 1.874x + 0.304x^2 \quad (\text{for } x > 0.3) \quad (2)$$

These relations are plotted in Fig.2. We estimate $\Delta E_c(x)$ using Stern's model¹⁵ of a single heterojunction with fixed barrier height, V_b , under flat band conditions at equilibrium,

$$V_b = E_0 + E_f + E_{db} + V_l + V_{sp} \quad (3)$$

where E_0 is the first subband energy measured from the bottom of the QW, E_f is the Fermi energy, E_{db} is the donor binding energy, V_l and V_{sp} are, respectively, the potential drops in the electron supply layer and the spacer layer.

At 300 K the shallow Si donor levels which lie about 5 meV below the conduction band of $\text{In}_y\text{Al}_{1-y}\text{As}$ are ionized; however, electrons associated with deep donor levels must also be considered. Because our growth conditions are similar to those of Higuchi et al.¹⁶ we choose $E_{db}=0.34$ eV as the appropriate level and assign an error bar of ± 0.1 eV to include discrepancies with other reported values¹⁷⁻¹⁹ in the range between 0.25 eV and 0.39 eV. We have used eq.(3), in conjunction with Fig.1 to calculate the dependence of ΔE_c on x shown in Fig.2.

Also included here is the reported ΔE_c of the lattice matched alloy¹²

$\text{In}_{0.52}\text{Al}_{0.48}\text{As}/\text{In}_{0.53}\text{Ga}_{0.47}\text{As}$ grown on InP. These data suggest that for both the direct and the indirect compositions of $\text{In}_y\text{Al}_{1-y}\text{As}$, $\Delta E_c \sim 0.67\Delta E_g$; and that for $x=0.3$ the conduction band offset is larger than that of the lattice matched alloy grown on InP. We do not have a satisfactory explanation why the maximum n_s occurs at $x=0.4$ rather than at $x=0.3$, as shown in Fig.2. While a similar change of $n_s(x)$ was reported by Hsu et al.²⁰ on δ -doped, pseudomorphic $\text{In}_x\text{Ga}_{1-x}\text{As}/\text{GaAs}$

heterostructures, we believe that the change in the energy differences between the Fermi level and the subbands as a function of x , due to quantum size effects, is responsible for their observations.

Figure 3 shows the composition dependence of μ , determined from Hall and resistivity measurements, made at 300 K and 77 K. At room temperature, μ increases by about 14%, from $9 \times 10^3 \text{ cm}^2/\text{V-s}$ for $x=0.07$ to $1.05 \times 10^4 \text{ cm}^2/\text{V-s}$ for $x=0.45$. For comparison purpose, a typical²¹ modulation doped, lattice matched heterojunction grown on InP with the same n_s , has $\mu(300 \text{ K}) = 1.2 \times 10^4 \text{ cm}^2/\text{V-s}$ and $\Delta E_c = 0.5 \text{ eV}$. The pseudomorphic structures described by Hsu et al.²⁰ have considerably smaller mobilities, the highest being $\mu(300 \text{ K}) = 5.5 \times 10^3 \text{ cm}^2/\text{V-s}$ for $x=0.37$, due perhaps, to interface roughness scattering.

In our case, the effective mass enhancement at the Fermi level, after accounting for the non-parabolicity of the conduction band,²² leads to a reduction of m^* from 0.068 to 0.057, for the same composition range. This 16% decrease in m^* might account for the experimentally observed increase in μ with x . While the composition dependence of μ at room temperature is weak, and is dominated principally by polar optical phonon scattering, this dependence is much stronger at 77 K as shown in Fig.3. We assume that in this instance while additional processes such as impurity scattering, deformation potential scattering and piezoelectric scattering are present, the measured $\mu(x)$ is dominated by alloy scattering. As shown by Saxsena,²³ the alloy scattering limited mobility μ_{AL} is proportional to $1/m^{*5/2}x(1-x)$. A superposition of the various scattering mechanisms, including the non-parabolicity of the conduction band, leads to a minimum in μ occurring at $x \sim 0.38$ in accordance with the experimental measurements as shown in fig.3. Figure 3 also includes some data of Inoue et al.²⁴ obtained on lattice matched $\text{In}_x\text{Ga}_{1-x}\text{As}/\text{In}_y\text{Al}_{1-y}\text{As}$ heterostructures similar to ours, but grown on GaAs substrates using linearly graded composition buffer layers. Their values are somewhat smaller than ours attributed here to a larger ionized impurity scattering induced by a factor of two greater impurity concentration in the supply layer and a spacer layer which is only 3 nm in thickness. We conclude, tentatively, that there is

no particular advantage for choosing a linearly graded over a stepwise graded buffer layer for producing effectively strain relaxation by means of buffer layers.

Fig. 3 also shows, for comparison purpose, the electron mobilities²⁵ of a pseudomorphic, δ -doped, $\text{Al}_{0.35}\text{Ga}_{0.65}\text{As}/\text{In}_{0.17}\text{Ga}_{0.83}\text{As}$ heterojunction (represented by triangular symbols) made in essentially the same configuration as that of the strain-relaxed heterostructures. Its $\mu(300\text{ K}) = 9.3 \times 10^3 \text{ cm}^2/\text{V-s}$ is about 7% smaller than that of similar strain-relaxed structure while at 77 K its mobility, $\mu(77\text{ K}) = 4.21 \times 10^4 \text{ cm}^2/\text{V-s}$ is about 20% smaller than that of strain relaxed structures.

In summary, we have measured n_s and μ of the 2DEG in strain relaxed $\text{In}_y\text{Al}_{1-y}\text{As}/\text{In}_x\text{Ga}_{1-x}\text{As}$ ($x < 0.45$) heterojunctions, with the same Si doping concentration in the carrier supply layer and the same device configuration. The dependence of n_s on x of these heterostructures is attributed to composition dependent $\Delta E_g(x)$, with $\Delta E_c \sim 0.67 \Delta E_g$. The maximum in $\Delta E_c = 0.72 \text{ eV}$ is deduced for $\text{In}_{0.29}\text{Al}_{0.71}\text{As}$, at $x=0.3$. At room temperature the electron mobility increases slightly with x , from $9 \times 10^3 \text{ cm}^2/\text{V-s}$ for $x=0.07$ to $1.05 \times 10^4 \text{ cm}^2/\text{V-s}$ for $x=0.45$; while at 77 K, a strong composition dependence of the electron mobility, dominated by alloy scattering, leads to a minimum of $\mu(x)$ near $x=0.4$.

References

- ¹S. Adachi, Properties of Indium Phosphide, (The Institution of Electrical Engineers, London, 1991), EMIS Datareview Series No.6, p.390
- ²J.-P. Reithmaier, R. Hoyer, H. Riechert, A. Heberle, G. Abstreiter and G. Weimann, Appl. Phys. Lett. 56, 536 (1990)
- ³G. Ji, D. Huang, U.K. Reddy, T.S. Henderson, R. Houdre and H. Morkoc, J. Appl. Phys. 62, 3366 (1987)
- ⁴J.W. Matthews and A.E. Blakeslee, J. Cryst. Growth 27, 118 (1974)
- ⁵S.L. Weng, J. Appl. Phys. 66, 2217 (1989)
- ⁶T.G. Andersson, Z.G. Cheng, V.D. Kulakovskii, A. Uddin and J.T. Vallin, Solid State Commun. 64, 379 (1987)
- ⁷N. Debbar, D. Biswas and P. Bhattacharya, Phys. Rev. B 40, 1058 (1989)
- ⁸C.T. Liu, S.Y. Lin, and D.C. Tsui, Appl. Phys. Lett. 53, 2510 (1988)
- ⁹J.L. Thobel, L. Baudry, A. Cappy, P. Bourel and R. Fauquembergue, Appl. Phys. Lett. 56, 346 (1990)
- ¹⁰D.J. Arent, K. Deneffe, C. Van Hoof, J. De Boek and G. Borghs, J. Appl. Phys. 66, 1739 (1989)
- ¹¹J.C.P. Chang, J. Chen, J.M. Fernandez, H.H. Wieder and K.L. Kavanagh, Appl. Phys. Lett. 60, 1129 (1992)
- ¹²J.R. Waldrop, E.A. Kraut, C.W. Farley and R.W. Grant, J. Appl. Phys. 69, 372 (1991)
- ¹³R.E. Nahory, M.A. Pollack, W.D. Johnston Jr. and R.A. Barns, Appl. Phys. Lett. 33, 659 (1978)
- ¹⁴B. Wakefield, M.A.G. Halliwell, T. Kerr, D.A. Andrews, G.J. Davies, and D.R. Wood, Appl. Phys. Lett. 44, 341 (1984)
- ¹⁵F. Stern, Appl. Phys. Lett. 43, 974 (1983)

- ¹⁶M. Higuchi, T. Ishikawa, K. Imanishi and K. Kondo, J. Vac. Sci. Technol. B 9, 2802 (1991)
- ¹⁷M.A. Tishler, B.D. Parker, P.M. Mooney and M.S. Goorsky, J. Electron. Mater. 20, 1053 (1991)
- ¹⁸P.S. Whitney, W. Lee and C.G. Fonstad, J. Vac. Sci. Technol. B 5, 796 (1987)
- ¹⁹W.P. Hong, S. Dhar, P.K. Bhattacharya and A. Chin, J. Electron. Mater. 16, 271 (1987)
- ²⁰W.C. Hsu, C.M. Chen and W. Lin, J. Appl. Phys. 70, 4332 (1991)
- ²¹H.T. Griem, K.H. Hsieh, I.J. D'Haenens, M.J. Delaney, J.A. Henige, G.W. Wicks and A.S. Brown, J. Vac. Sci. Technol. B 5, 785 (1987)
- ²²T. Ando, Jpn. J. Appl. Phys. 51, 3893 (1983)
- ²³A.K. Saxena, Phys. Rev. B 24, 3295 (1981)
- ²⁴K. Inoue, J.C. Harmand and T. Matsuno, J. Cryst. Growth, 111, 313 (1991)
- ²⁵J.M. Fernandez, J. Chen and H.H. Wieder, J. Vac. Sci. Technol. B10, 1992, to be published.

Figure captions

FIG. 1. Electron sheet density n_s of strain relaxed $\text{In}_y\text{Al}_{1-y}\text{As}/\text{In}_x\text{Ga}_{1-x}\text{As}$ modulation doped heterojunctions as a function of indium composition measured at $T=300$ K. The nominal Si doping concentration in the $\text{In}_y\text{Al}_{1-y}\text{As}$ carrier supply layer is $1 \times 10^{18} \text{ cm}^{-3}$.

FIG. 2. Conduction band discontinuity ΔE_c of lattice matched $\text{In}_y\text{Al}_{1-y}\text{As}/\text{In}_x\text{Ga}_{1-x}\text{As}$ heterostructures. The open circle is data from ref.12. The solid lines are the band gap energy differences between the two lattice matched ternaries and the dashed lines represent 67% of the band gap energy differences.

FIG. 3. Electron mobilities of modulation doped $\text{In}_y\text{Al}_{1-y}\text{As}/\text{In}_x\text{Ga}_{1-x}\text{As}$ heterojunctions at room temperature and at 77 K. The open squares are from Inoue et al. (ref. 24) The triangles are from a pseudomorphic $\text{Al}_{0.35}\text{Ga}_{0.65}\text{As}/\text{In}_{0.17}\text{Ga}_{0.83}\text{As}$ sample. The dashed curves are guide to the eye.

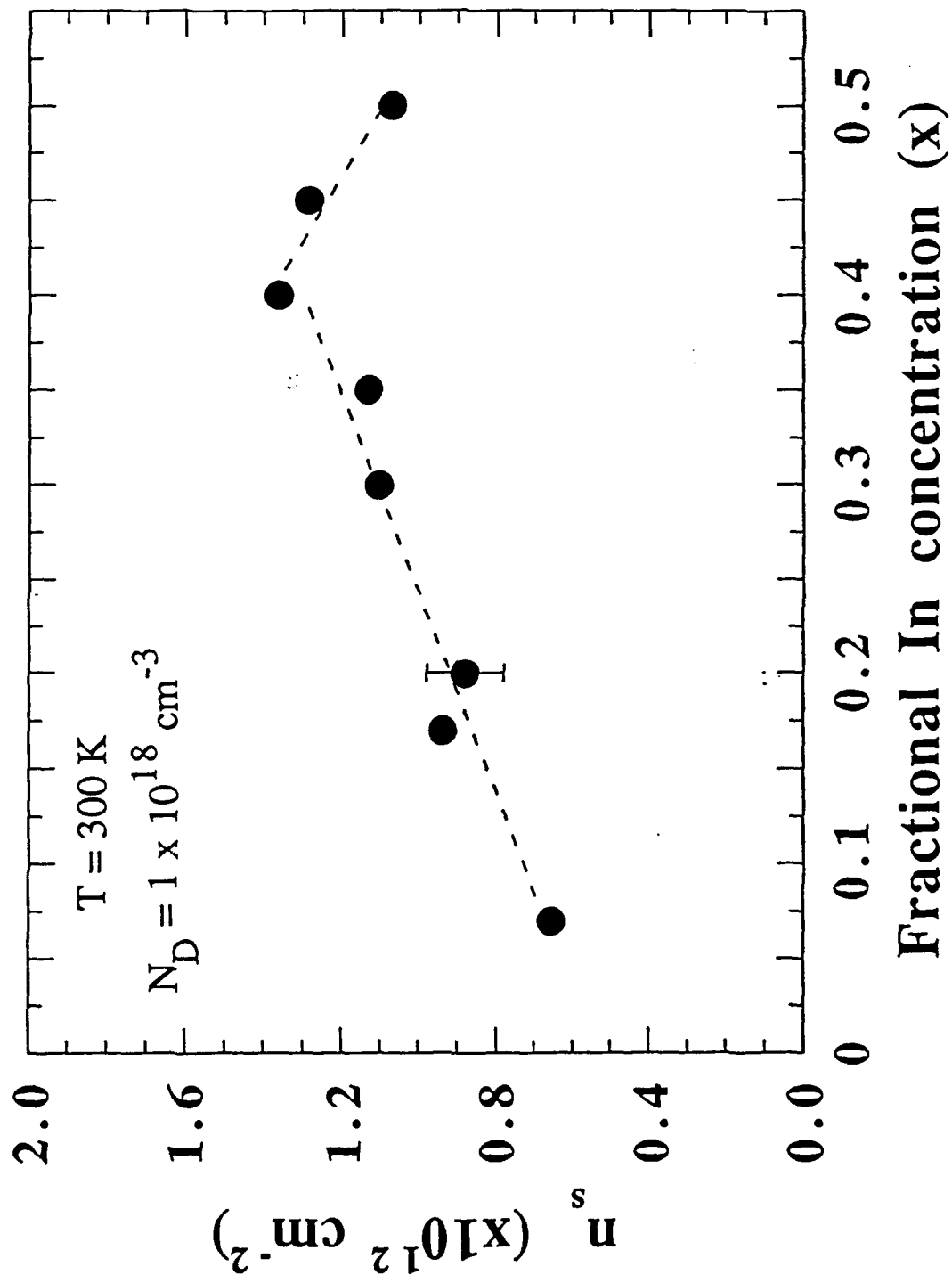


Fig. 1 of 3

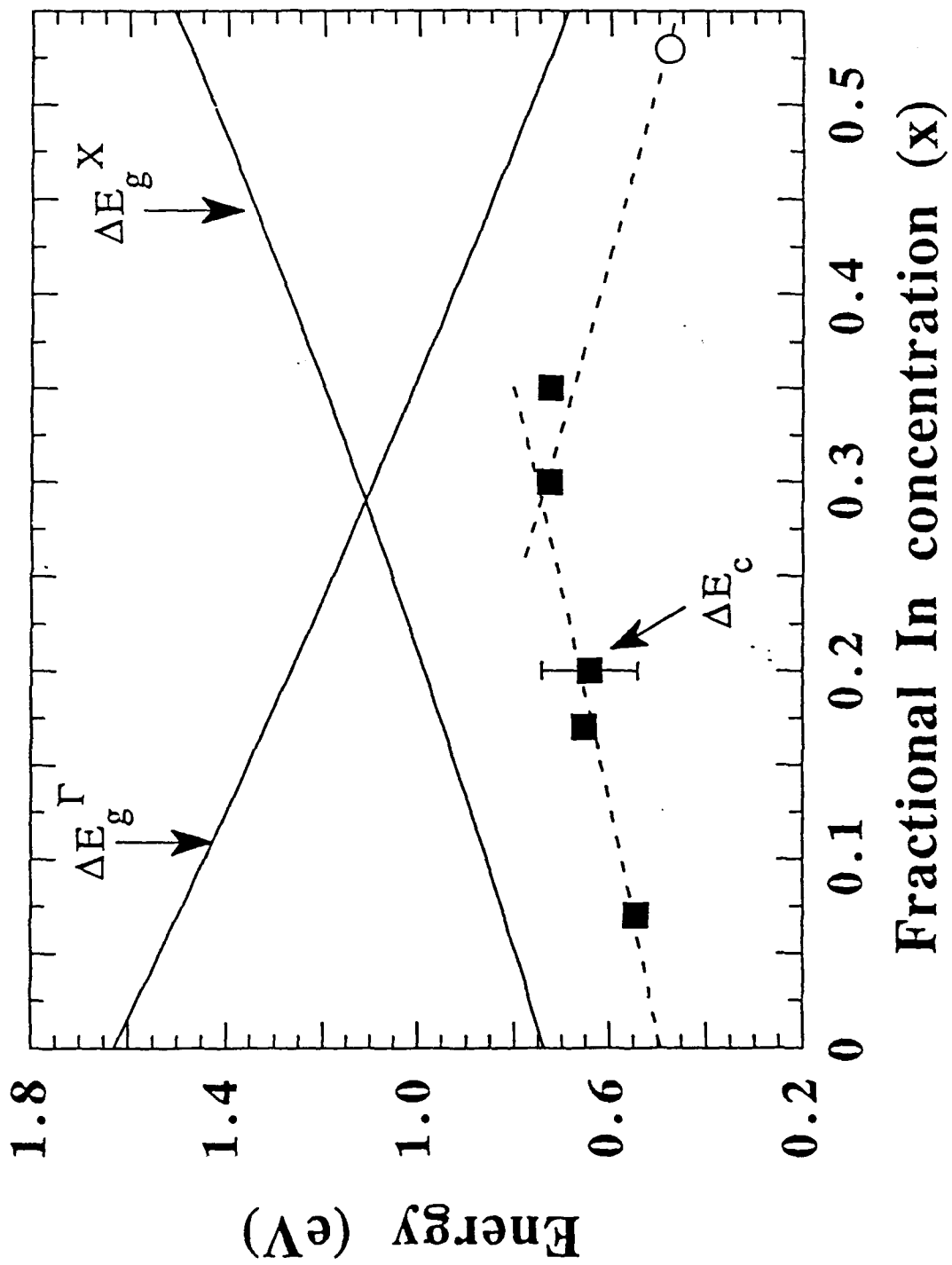


Fig. 2 of 3

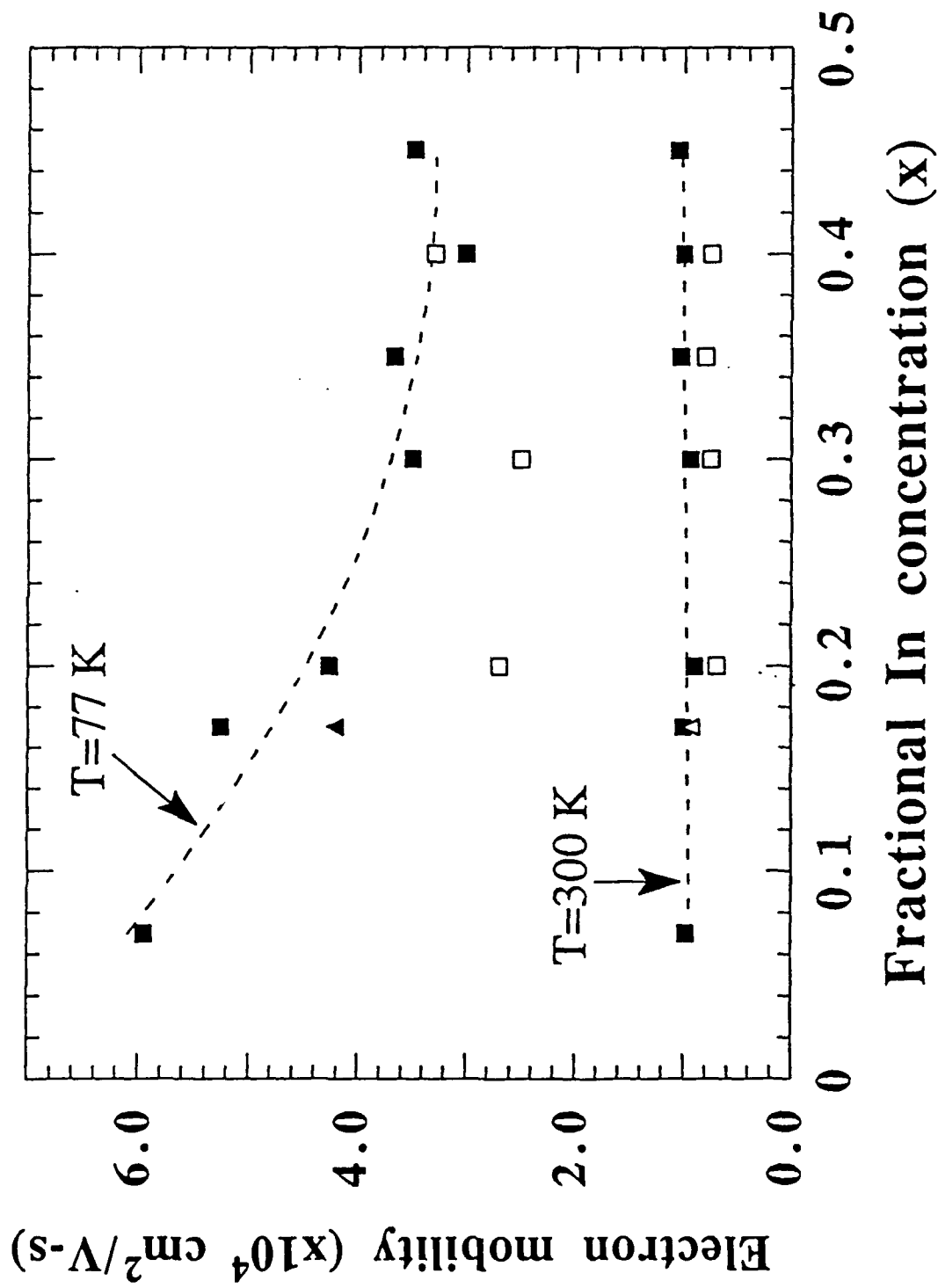


Fig. 3 of 3

APPENDIX 4

accepted for publication in J.Vac.Sci.Technol.B10, July/August(1992)

3/22/92

used

19 for

JVS T

Lattice Tilt and Dislocations in Compositionally Step-Graded Buffer Layers for Mismatched InGaAs/GaAs Heterointerfaces

K. L. Kavanagh, J. C. P. Chang, J. Chen, J. M. Fernandez, and H.H. Wieder

Department of Electrical and Computer Engineering,

University of California at San Diego, La Jolla, CA 92093-0407

The strain relaxation and dislocation densities of a compositionally step-graded InGaAs/GaAs buffer layer have been investigated. The structural results were correlated with the electrical properties of an $\text{In}_{0.3}\text{Ga}_{0.7}\text{As}/\text{In}_{0.29}\text{Al}_{0.71}\text{As}$ modulation doped heterostructure grown on top. The buffer was a three step $\text{In}_x\text{Ga}_{1-x}\text{As}$ structure each layer 300 nm thick and each In composition step $x = 0.1$. X-ray rocking curve analysis measured a tilt about an in-plane $\langle 110 \rangle$ axis of about 0.3° per step. At the top interface of the buffer the density of misfit dislocations evaluated by electron microscopy was comparable to the number required to account for this tilt. Thus, the 60° burgers vectors for the majority of dislocations along one in-plane line direction was restricted to a maximum of two rather than the usual four possibilities. The electron mobility in the two-dimensional electron gas channel showed a small assymetry (4%) in the two in-plane $\langle 110 \rangle$ directions and was highest in the direction parallel to the tilt axis. The sheet electron concentration was $1.2 \times 10^{12}/\text{cm}^2$ with peak mobilities of 9300 and 31,000 $\text{cm}^2/\text{V-s}$ at room temperature and 77K, respectively.

I. INTRODUCTION

Strain relaxation of lattice mismatched semiconductor epilayers occurs by the formation of dislocations at the interface. Necessarily associated with this process is the generation of threading dislocations in the bulk of the epilayers which may or may not glide and annihilate at the edge of the sample. It is well known that partially relaxed single epilayer material with relatively few threading dislocations can be grown as long as the lattice mismatch is not too large and the growth process sufficiently clean. Specifically, in the case of $\text{In}_x\text{Ga}_{1-x}\text{As}/\text{GaAs}$, if the In mole fraction, x , is less than about 0.18 (1.25% mismatch) then the threading dislocation density in a single epilayer can be less than the lower limit detectable by plan-view transmission electron microscopy (TEM) about $10^6/\text{cm}^2$.^{1,2} With In compositions greater than $x = 0.18$ the surface becomes increasingly rougher with the eventual onset of three dimensional growth leading to island formation and sessile edge dislocation generation.³ The resulting material is badly dislocated with densities greater than $10^8/\text{cm}^2$.

Therefore, in order to grow low defect density unstrained epitaxial layers on strongly mismatched substrates, buffer structures grown between the substrate and the surface epilayers are being investigated. Ideally, this buffer structure must be such that the relaxation of interfacial strains is contained within it and all threading dislocations glide to the edges of the sample rather than ending in the desired epitaxial layer. Although various strategies have been applied in the past a number of old and recent reports indicate that linearly or step-graded compositional buffer layers can be very effective for achieving such goals.⁴⁻⁹

We are investigating, in particular, the use of a compositionally step graded $\text{In}_x\text{Ga}_{1-x}\text{As}$ buffer layer for the growth of modulation doped $\text{In}_x\text{Ga}_{1-x}\text{As}/\text{In}_y\text{Al}_{1-y}\text{As}$ heterostructures on GaAs substrates. This type of buffer layer is easy to grow reliably in our molecular beam epitaxy (MBE) system and the analysis of strain relaxation in each layer of the buffer is feasible by high resolution x-ray diffraction. Also, the two-dimensional electron gas (2-DEG) present in the modulation-doped $\text{In}_x\text{Ga}_{1-x}\text{As}$ layer offers a means to

correlate the electrical properties with the composition, strain, microstructure and dislocation densities determined by x-ray diffraction and TEM. We have chosen a step size of $x = 0.1$ and a layer thickness of 300 nm based on published reports^{8,9} and our own earlier work with single epilayers.² This has proven quite successful, so far, for In compositions up to $x \leq 0.3$ (three layer buffer).¹⁰ In this paper we emphasize the relationship between the epilayer tilt measured by x-ray diffraction and misfit dislocation densities observed with TEM.

II. EXPERIMENTAL DETAILS

Samples were grown by molecular beam epitaxy, on (001)-oriented GaAs substrates cut 2° off towards the [010] direction. The structures consisted of an initial 200 nm thick undoped GaAs layer, followed by a 3-step graded buffer layer consisting of undoped, 300 nm thick $\text{In}_x\text{Ga}_{1-x}\text{As}$ layers with nominal In mole fractions of $x = 0.1, 0.2$ and 0.3 . Superposed on this buffer layer is a 10 nm thick, undoped $\text{In}_{0.29}\text{Al}_{0.71}\text{As}$ spacer layer, a 30 nm Si-doped ($N_d = 1 \times 10^{18} / \text{cm}^3$) $\text{In}_{0.29}\text{Al}_{0.71}\text{As}$ charge supply layer and topmost is a 10 nm Si-doped ($N_d = 3 \times 10^{17} / \text{cm}^3$) GaAs cap layer. The substrate temperature was kept at 535°C for all layers. We have two In cells and thus there were no unusual delays between growth at each composition step.

Cross-sectional TEM was carried out on epoxied samples thinned by Ar ion-milling (5 keV) at liquid nitrogen temperature. Plan-view samples were prepared by chemical etching from the substrate side. All TEM was carried out using a Philips CM30 at an accelerating voltage of 300 keV.

The alloy composition and layer strains were measured with a high resolution x-ray diffractometer using $\text{CuK}\alpha_1$ radiation. There proved to be a large tilt in each of the epilayers with respect to the substrate. Thus (004) and (224) rocking curves were recorded at eight azimuthal angles in order to obtain an accurate measure of this tilt.¹¹

III. RESULTS

A cross-sectional image of the sample taken near the [110] pole in a two beam (004) condition is shown in Fig. 1 (a). The dislocation density and morphologies are similar at each interface comparable to earlier observations with single heterointerfaces.² Dislocation loops are seen inside the substrate and in the first two layers of the buffer. By tilting the sample about the [001] axis perpendicular to the plane of the film, loops orientated in the perpendicular [011] direction are elongated and become more visible. Figure 1 (b) shows the same area as (a) tilted 45° to the [010] pole in a (004) two beam condition. Multiple loops stacked above each other are often visible possibly originating from the same source at the interface. The top layer of the buffer is devoid of any threading dislocations in this image and in all thin regions of the TEM sample.

Plan-view micrographs of this sample are shown in Fig. 2. Both the loops and the in-plane dislocations seen in these micrographs have 60° burgers vectors of type $a/2\langle 110 \rangle$. The parallel dislocations running in only one $\langle 110 \rangle$, actually the $[-110]$ direction, are associated with the InAlAs/InGaAs 2-DEG interface. These indicate that there was a small lattice mismatch between these two layers unintentionally introduced during growth. The reason for the nucleation in only one direction at low mismatch has been attributed to differences in the nucleation rate and velocities of Ga and As core dislocations¹⁴. We will argue that it may also be due to preferential slip planes resulting from the substrate surface offcut.¹⁵ The density of these dislocations is $1 \times 10^4/\text{cm}$ corresponding to a strain relaxation of only 0.02% for 60° dislocations. No dislocations were observed in the surface regions of the sample next to the etched hole. The sampling area of $135 \mu\text{m}^2$ gives an upper limit to the threading dislocation density of $7 \times 10^5/\text{cm}^2$. The orthogonal array of misfit dislocations is associated with the $\text{In}_{0.2}\text{Ga}_{0.8}\text{As}/\text{In}_{0.3}\text{Ga}_{0.7}\text{As}$ interface. The density is $2.0 \times 10^5/\text{cm}$ and $1.6 \times 10^5/\text{cm}$ in the two perpendicular in-plane [110] directions. For 60° dislocations this corresponds to a strain relaxation of 0.4 and 0.32%, respectively. These values should be compared with the misfit between the two buffer layers, 0.7%. Thus, the dislocation

densities indicate that the top buffer layer is relaxed by 45 and 57%, respectively, consistent with our experience with single heterointerfaces.²

X-ray rocking curves from the (004) and (224) reflections are shown in Fig. 3. With the x-ray beam parallel the [110] direction, rotation angle $\omega = 0^\circ$, each epilayer peak is resolved. But after a rotation about the plane normal, [001], by 180° all three peaks have overlapped with the substrate peak. The only explanation for this is that the films are tilted about the in-plane [-110] axis by a value comparable to the Bragg angle difference, $\Delta\theta_B$. Further analysis of the data shows that the tilts and hence $\Delta\theta_B$ for the $x = 0.3$ and 0.2 layers are 0.85° and 0.55° , respectively. The tilt in the first layer could not be independently obtained from this data but, considering the results from the two other layers, its tilt is likely between 0.25 and 0.3° .

From combined analysis of both sets of rocking curves, the composition of the third layer was confirmed to be close to 0.3 , i.e., 0.31 ± 0.01 . Its residual in-plane strains, ϵ^r , defined as $(a_{110} - a_f)/a_f$ were calculated to be -0.33 and -0.04% , for the [110] and [-110] directions, respectively, a large asymmetry.¹⁰ Therefore, with respect to a relaxed second buffer layer the relaxation of buffer layer three was 52 and 94%, respectively.

But, another way to look at this data is to compare the residual strain of layer three with respect to the substrate misfit. The lattice misfit between layer three and the substrate is 2.23%. Thus, 85 and 98% of the misfit between layer 3 and the substrate has been relaxed in the two perpendicular directions. Further confirmation of the low absolute strain in the third buffer layer was obtained by etching off the 2-DEG structure from a similar step-graded wafer and measuring the photoluminescence response at 10K as a function of wavelength. The peak response occurred at an energy of 1.1 eV (3.4 nm FWHM) in close agreement with 1.09 eV, that of bulk unstrained $\text{In}_{0.3}\text{Ga}_{0.7}\text{As}$.

Finally, the electron mobility, μ , in the 2-DEG channel measured along the two orthogonal $\langle 110 \rangle$ directions as a function of temperature is plotted in Fig. 4. At 77K the electron mobility derived from Hall and resistivity measurements is $\mu = 3.1 \times 10^4 \text{ cm}^2/\text{V-s}$

and $2.96 \times 10^4 \text{ cm}^2/\text{V-s}$ respectively, a 4% asymmetry. The corresponding room temperature mobilities were $\mu = 9340 \text{ cm}^2/\text{V-s}$ and $8990 \text{ cm}^2/\text{V-s}$. In each case the highest mobility direction occurred in the $[-110]$ direction parallel to the dislocations at the 2-DEG interface. Assuming the 77K mobility to be limited principally by remote impurity scattering, alloy scattering and polar optical phonon scattering, the estimated 2 DEG mobility present in unstrained $\text{In}_{0.3}\text{Ga}_{0.7}\text{As}$ for the same supply layer doping and device configuration is $\mu = 4 \times 10^4 \text{ cm}^2/\text{V-s}$. The lower mobility and the anisotropy of the experimental results is attributed here to the 7% residual strain asymmetry (with respect to the substrate), to threading dislocations (at a density not greater than $1 \times 10^6/\text{cm}^2$), and to the asymmetric misfit dislocations. Dislocations running perpendicular to the transport direction add a scattering component to the mobility limiting mechanism. ~~And because of the small~~ asymmetry in mobility with the large asymmetry in the misfit dislocations density at the 2-DEG interface we suspect that the misfit dislocations are ^{more} less important than the threading dislocations. We estimate the mobility component associated with scattering by ^{misfit} ~~threading~~ dislocations to be of the order $10^5 \text{ cm}^2/\text{V-s}$.

IV. DISCUSSION

A large tilt detected by x-rays has been noticed before in single $\text{GaInAs}/\text{GaAs}$ heterointerfaces and in other lattice mismatched systems.^{11,15-16} The tilt is thought to originate from a combination of two effects. The first is the geometrical effect of the surface steps first considered by Nagai.¹⁶ This tilt would be present in both pseudomorphic and partially relaxed epilayers and would occur about an axis parallel to the surface offcut tilt axis but in the opposite direction. The second effect is the result of plastic deformation when the generation of misfit dislocations results in a net burgers vector component perpendicular to the interface. The geometrical tilt effect as predicted by Nagai in our case for a $\text{In}_{0.3}\text{Ga}_{0.7}\text{As}/\text{GaAs}$ sample grown on a 2° offcut surface would contribute a tilt of 152

arcsecs, small compared with the tilt measured, 3060 arcsecs. Furthermore, this tilt would be a rotation about the [010] axis 45° to the tilt axis we measured.

Considering the dislocation contribution we can easily calculate how many interfacial dislocations must be contributing towards the tilt in the films. The tilt between the second and third buffer layer was 0.3° . Each 60° misfit dislocation has an edge component perpendicular to the plane of the interface equal to $a/2[001]$ with a magnitude of $a/2$. Therefore, the dislocation spacing necessary to account for this tilt is given by $a/2\sin(0.3^\circ)$ which equals 55 nm/dislocation or $1.8 \times 10^5/\text{cm}$. Interestingly, this number is comparable to the dislocation density observed by TEM ($1.6 \times 10^5/\text{cm}$) indicating that in the $[-110]$ line direction possibly all of the dislocations were restricted to only two of the possible four burgers vectors. With a little more TEM work we might be able to confirm this result. It would also be interesting to check for a rotation in the film about the [001] direction and thus determine if the dislocations are limited to only one burgers vector.

The reason for the preferential formation of only one or two burgers vectors can be due to a preference for particular glide planes forced by the offcut tilt in the surface.¹⁵ Alternatively, a dislocation multiplication process is operating which has a preference for one or two types of Burgers vectors. Further investigations are required.

To summarize our results the directions of each of the phenomena observed is shown in the diagram in Fig. 5. The tilt axis along $[-110]$ is 45° to that of the offcut axis along [100]. The geometrical effect of the offcut on the tilt is negligible on the scale of tilt measured here. The highest mobility occurs in the direction parallel to the tilt axis which is also the line direction of the dislocations at the 2-DEG interface. The tilt axis is also parallel to the line direction of the dislocations with the lower density at the interface between the second and third buffer layers. Therefore, the maximum strain relaxation occurred in the $[-110]$ direction, parallel to the tilt axis.

V. CONCLUSIONS

We have correlated to first order the residual strain present in a compositionally step-graded InGaAs buffer layer with the electrical properties of a modulation doped $\text{In}_{0.3}\text{Ga}_{0.7}\text{As}/\text{In}_{0.29}\text{Al}_{0.71}\text{As}$ heterostructure grown upon it. X-ray data showed that the top buffer layer misfit with respect to the substrate was, on average, 91% relaxed with a 7% asymmetry in the two in-plane $\langle 110 \rangle$ directions. Each layer of the buffer was tilted by about 0.3° with respect to its neighbors about the in-plane $[-110]$ axis. This tilt corresponds to a misfit dislocation density approximately equal to the density measured by plan-view TEM. Thus, in the $[-110]$ in-plane direction the misfit burgers vectors are restricted to only 1 or 2 possibilities. Further work is required to understand the significance of this result to the underlying dislocation nucleation mechanisms in this material. The 2-DEG channel had a sheet electron density of $1.2 \times 10^{12}/\text{cm}^2$, peak mobilities of $9300 \text{ cm}^2/\text{V-s}$ at room temperature and $31,000 \text{ cm}^2/\text{V-s}$ at 77K with a mobility anisotropy of 4%.

ACKNOWLEDGEMENTS

This work was supported in part by NSF and the Naval Research Laboratory (N. Wilsey). KK thanks F. LeGoues (IBM) for many useful discussions.

- ¹ V. Krishnamoorthy, P. Ribas, R.M. Park, Appl. Phys. Lett. **58**, 2000 (1991).
- ² K.L.Kavanagh, M.A. Capano, L.W. Hobbs, J.C. Barbour, P.M.J. Maree, W. Schaff, J.W. Mayer, D. Pettit, J.M. Woodall, J.A. Strosio and R.M. Feenstra, J. Appl. Phys. **64**, 4843 (1988).
- ³ M. Lentzen, D. Gerthsen, A. Forster, K. Urban, Appl. Phys. Lett. **60**, 74 (1992).
- ⁴ M.S. Abrahams, I.R. Weisberg, C.J. Buiocchi, J. Blanc, J. Mat. Sci. **4**, 223 (1969).
- ⁵ G.H. Olsen, M.S. Abrahams, C.J. Buiocchi, T.J. Zamerowski, J. Appl. Phys. **46**, 1643 (1975).

- ⁶ E.A. Fitzgerald, Y.-H. Xie, M.L. Green, D. Brasen, A.R. Kortan, J. Michel, Y.-J. Mii, B.E. Weir, Appl. Phys. Lett. ⁸ ~~59~~ ⁸ 3323 (1990).
- ⁷ F.K. LeGoues, B.S. Meyerson, J.F. Morar, Phys. Rev. Lett. **66**, 2903 (1991) and same authors plus P.D. Kirchner, J. Appl. Phys. **60**, 1129 (1992).
- ⁸ K. Chang, P. Bhattacharya, R. Lai, J. Appl. Phys. **67**, 3323 (1990).
- ⁹ K. Inoue, J.C. Harmand, T. Matsuno, J. Cryst. Growth, **111**, 313 (1991).
- ¹⁰ J.C.P. Chang, J. Chen, J.M. Fernandez, H.H. Wieder and K.L. Kavanagh, Appl. Phys. Lett. (unpublished).
- ¹¹ C.R. Wie, J. Appl. Phys. **65**, 2267 (1989).
- ¹² M.S. Abrahams, C.J. Buiocchi, G.H. Olsen, J Appl. Phys., **46**, 4259 (1975).
- ¹³ E.A. Fitzgerald, D.G.Ast, P.D. Kirchner, G.D. Petit, J.M. Woodall, J. Appl. Phys. **63**, 693 (1988).
- ¹⁴ M.S. Abrahams, J. Blanc, C.J. Buiocchi, Appl. Phys. Lett., **21**, 185 (1972).
- ¹⁵ J.E. Ayers, S.K. Ghandhi, L.J. Schowalter, J. Cryst. Growth, **113**, 430 (1991).
- ¹⁶ H. Nagai, **45**, 3789 (1974).

Figure Captions

Fig. 1 Cross-sectional transmission electron micrograph of a three step compositionally graded $\text{In}_x\text{Ga}_{1-x}\text{As}$ buffer layer grown on GaAs taken in a two-beam (004) condition (a) near a $\langle 110 \rangle$ pole and (b) tilted 45° to a $\langle 010 \rangle$ pole.

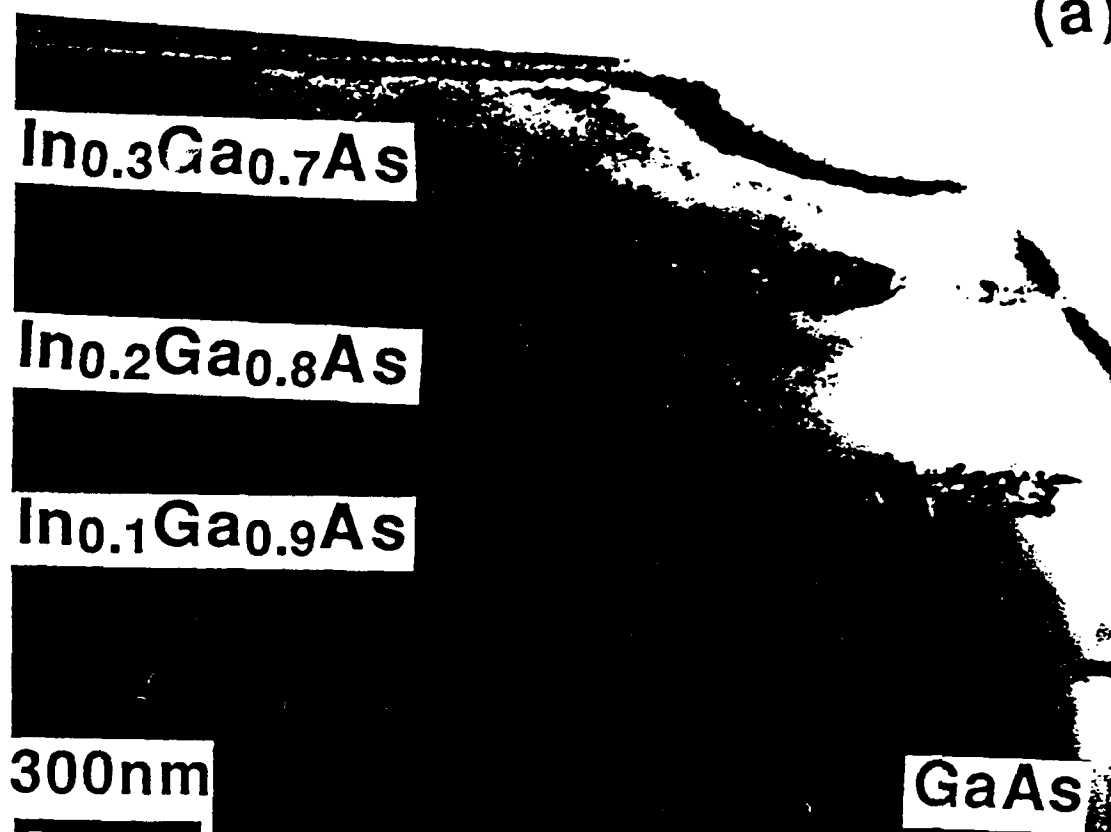
Fig. 2 Plan-view transmission electron micrograph of a three step compositionally graded $\text{In}_x\text{Ga}_{1-x}\text{As}$ buffer layer grown on GaAs. The sample is wedged shaped and therefore the two dimensional gas interface and the top interface of the buffer layer are distinguishable.

Fig. 3 (a) (004) and (b) x-ray rocking curves of a three step, compositionally step-graded $\text{In}_x\text{Ga}_{1-x}\text{As}$ buffer layer ($x = 0.1, 0.2$ and 0.3) taken for four azimuthal angles in 90° increments from $\omega = 0 - 270^\circ$.

Fig. 4 Hall mobilities and the sheet electron concentration of the channel of a $\text{In}_{0.3}\text{Ga}_{0.7}\text{As}/\text{In}_{0.29}\text{Al}_{0.71}\text{As}$ modulation doped heterostructure as a function of temperature and in-plane orientation.

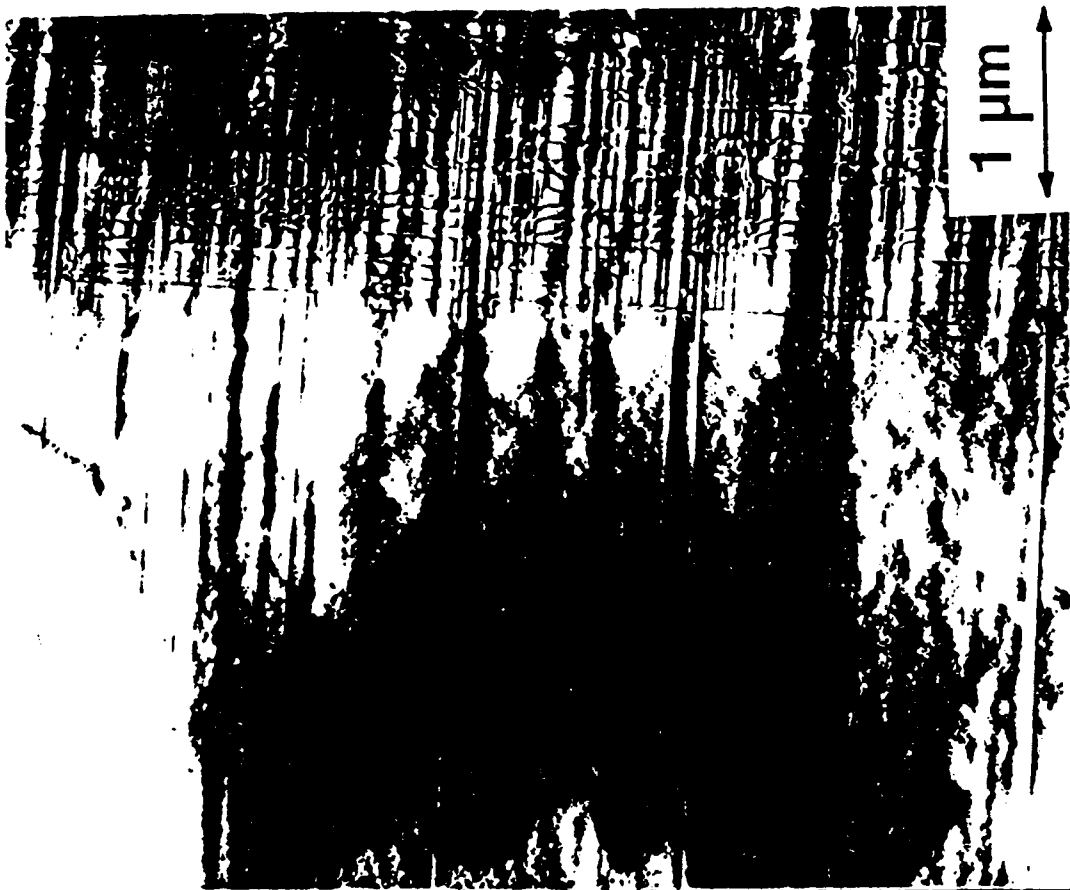
Fig. 5 Diagram showing the orientation of the epilayer tilt, interfacial dislocations and electron mobilities for a three layer step-graded $\text{InGaAs}/\text{GaAs}$ buffer.

(a)

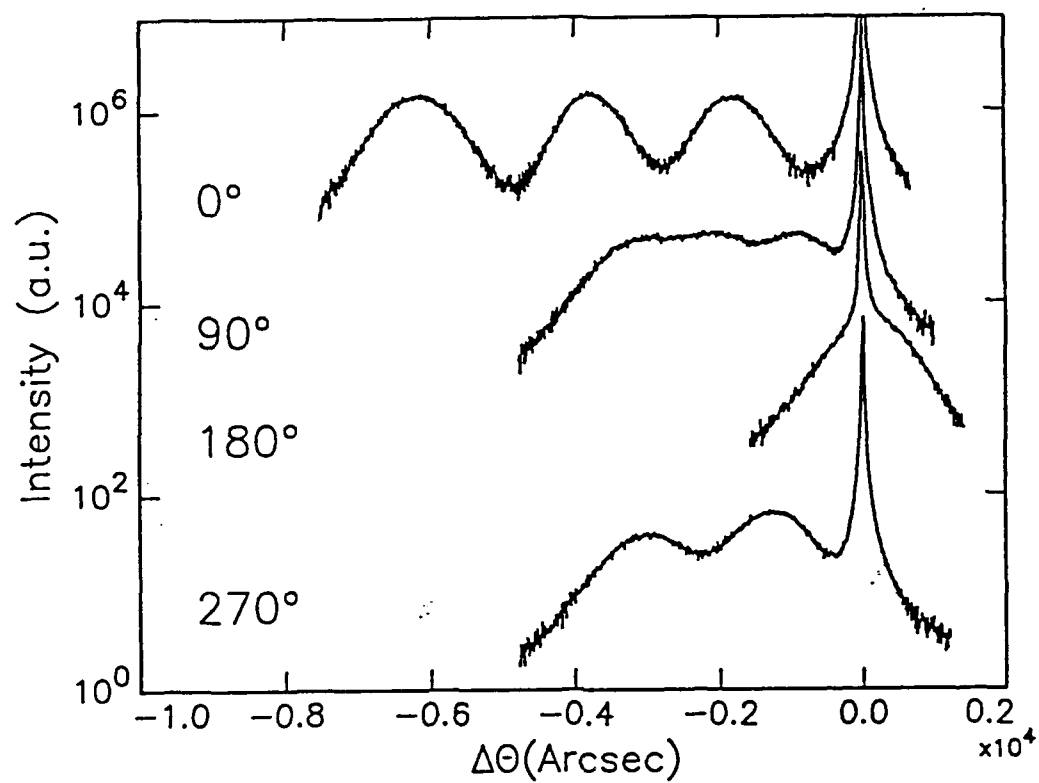


(b)

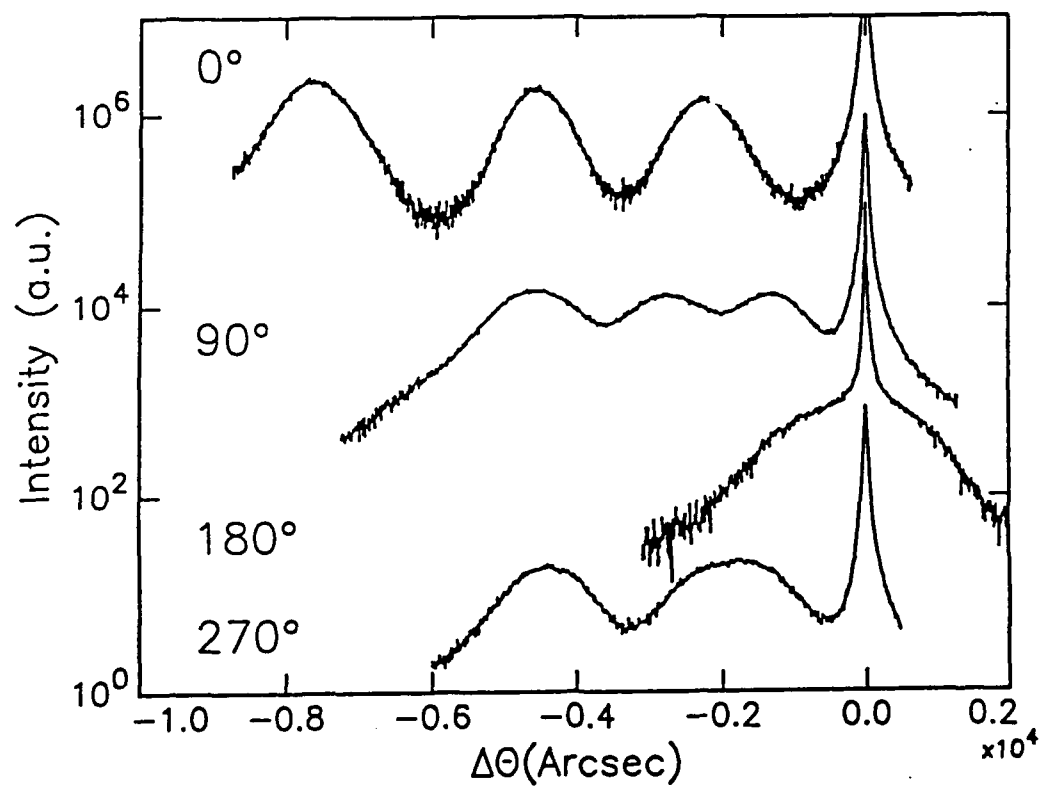




(a) (004)



(b) (224)



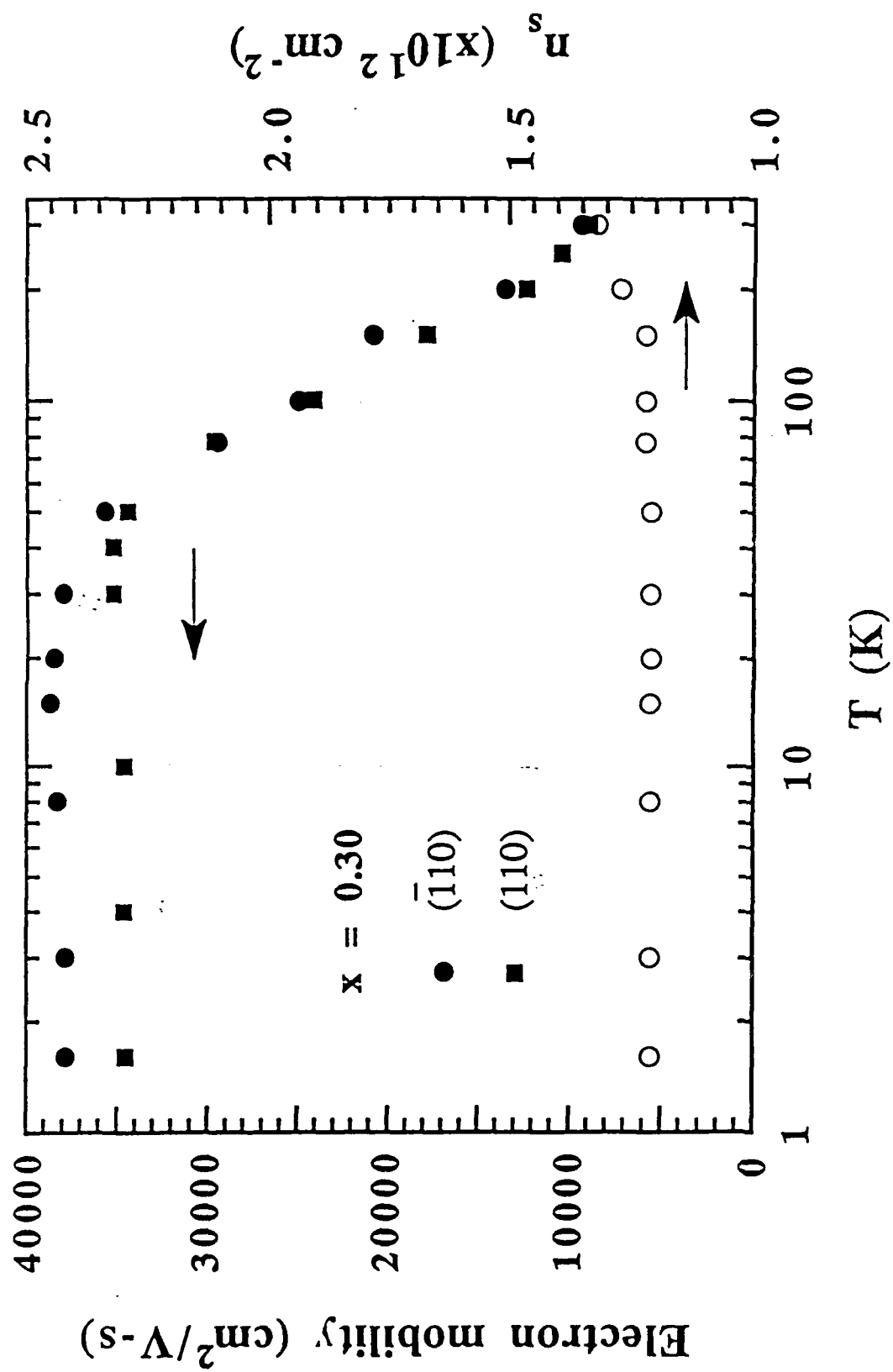
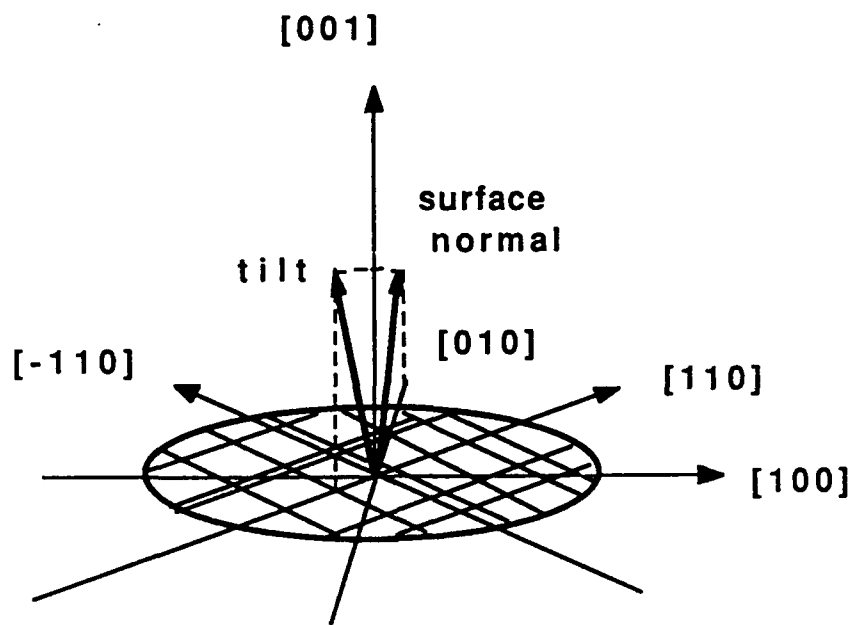


Fig. 4

Downloaded from



6/12/92

ANISOTROPIC ELECTRON MOBILITY OF
TWO-DIMENSIONAL-ELECTRON-GAS IN MODULATION DOPED
 $\text{In}_x\text{Ga}_{1-x}\text{As}/\text{In}_y\text{Al}_{1-y}\text{As}$ HETEROSTRUCTURES

Jianhui Chen, J.M. Fernandez, and H.H. Wieder
Electrical and Computer Engineering Department, 0407
University of California, San Diego
La Jolla, CA 92093-0407

ABSTRACT

We have investigated the electrical properties of the two-dimensional-electron-gas (2DEG) present in strain relaxed heterojunctions with $\text{In}_x\text{Ga}_{1-x}\text{As}$ channels ($x < 0.4$). These were grown by molecular beam epitaxy on misoriented (001) GaAs substrates using compositionally step graded buffer layers, $\Delta x' = 0.1$ per step, each step $0.3 \mu\text{m}$ thick. The 2DEG is produced by modulation doping using lattice matched $\text{In}_y\text{Al}_{1-y}\text{As}$ as the carrier supply layer. We find typical electron densities and mobilities, for $x=0.3$, of $n_s(300 \text{ K}) = 1.3 \times 10^{12} \text{ cm}^{-2}$ and $\mu_H(300 \text{ K}) = 9300 \text{ cm}^2/\text{V-s}$; and for $n_s(1.6 \text{ K}) = 1.2 \times 10^{12} \text{ cm}^{-2}$, $\mu_H(1.6 \text{ K}) = 37800 \text{ cm}^2/\text{V-s}$. While the room temperature electron mobility shows negligible anisotropy, an $\langle 110 \rangle$ -orientation dependent low temperature electron mobility of the 2DEG is observed and attributed to dislocation scattering.

INTRODUCTION

$\text{In}_x\text{Ga}_{1-x}\text{As}$ alloys are good candidates for high speed electronic devices because of their better transport properties including a higher electron mobility, and larger conduction band discontinuity when combined with other binary or ternary III-V semiconductors. However, their application is limited by a potentially large lattice mismatch when grown on GaAs substrate. Misfit strain causes elastic and plastic deformation of the $\text{In}_x\text{Ga}_{1-x}\text{As}$ lattices, which can degrade the transport properties of the epilayers. It is known that the low temperature electron mobility μ is sensitive to small numbers of dislocations,[1],[2] because other scattering mechanisms such as phonon and ionized impurity scatterings have much higher electron mobilities. Misfit dislocations are believed to be charged lines and therefore highly anisotropic scattering centers.[3],[4] For samples with a relatively small number of dislocations, their effect on electron transport properties is reflected in the anisotropy of the electron mobility as well as in a decrease of μ . Anisotropic transport properties were observed early in plastically deformed Germanium[5] and InSb[6]. Recently, anisotropic electron mobilities have been reported in single layers of $\text{In}_x\text{Ga}_{1-x}\text{As}$ grown on GaAs;[7],[8] in GaAs/ $\text{In}_{0.2}\text{Ga}_{0.8}\text{As}/\text{Al}_{0.3}\text{Ga}_{0.7}\text{As}$ inverted HEMT structures[9] for InGaAs layers both below and beyond the critical layer thickness. Orientation dependent device characteristics of lattice mismatched $\text{In}_x\text{Al}_{1-x}\text{As}/\text{In}_{0.53}\text{Ga}_{0.47}\text{As}$ HFET's grown on InP has also been reported.[10] These anisotropies were attributed to different dislocation densities in the two orthogonal $\langle 110 \rangle$ orientations. Sun et al.[11] also studied the effects of substrate misorientation on the anisotropic electron transport in InGaAs/GaAs heterostructures and found much higher μ and smaller anisotropy for samples grown on 2° off axis misoriented GaAs substrates.

The successful growth of strain relaxed $\text{In}_x\text{Ga}_{1-x}\text{As}$ provides additional advantages for device applications; these including the use of lattice matched $\text{In}_y\text{Al}_{1-y}\text{As}$ as the barrier layer which has a larger band offset with $\text{In}_x\text{Ga}_{1-x}\text{As}$ than $\text{Al}_y\text{Ga}_{1-y}\text{As}$ and GaAs[12] as well as the flexibility of choosing a specific bandgap energy and layer thickness. However strain relaxation

involves the formation of dislocations in numbers proportional to the mismatch. The effect of dislocations on the electron transport properties of strain relaxed $\text{In}_x\text{Ga}_{1-x}\text{As}$ epilayers is vital for device applications. In this work, we report the transport properties and the orientation-dependent electron mobilities of the two-dimensional-electron-gas (2DEG) in the strain relaxed, lattice matched $\text{In}_y\text{Al}_{1-y}\text{As}/\text{In}_x\text{Ga}_{1-x}\text{As}$ ($x < 0.4$) modulation doped (MD) heterojunctions grown by molecular beam epitaxy (MBE) on (001) mis-oriented GaAs substrates by means of compositionally step graded buffers. The higher electron mobilities and smaller degree of anisotropy compared to the 'quasi' pseudomorphic structures indicate the good crystalline quality and device applicability of such strain relaxed structures.

EXPERIMENT

The strain relaxed, lattice matched $\text{In}_y\text{Al}_{1-y}\text{As}/\text{In}_x\text{Ga}_{1-x}\text{As}$ heterojunctions were grown by MBE on (001) oriented GaAs substrates with a 2° offcut towards the nearest (110) plane. The two-dimensional-electron-gas present in the $\text{In}_x\text{Ga}_{1-x}\text{As}$ channel is produced by modulational doping with Si a 30 nm thick lattice matched $\text{In}_y\text{Al}_{1-y}\text{As}$ carrier supply layer which is separated from the channel layer by a 10 nm thick, undoped $\text{In}_y\text{Al}_{1-y}\text{As}$ spacer. The nominal Si doping concentration is $1 \times 10^{18} \text{ cm}^{-3}$ for all the samples. Interposed between the heterojunction and the GaAs substrate is a buffer composed of compositionally step graded $\text{In}_x'\text{Ga}_{1-x'}\text{As}$ or $\text{In}_x'(\text{Al}_y'\text{Ga}_{1-y'})_{1-x'}\text{As}$ layers. Each step is 300 nm thick with a composition increment, $\Delta x' = 0.1$ up to the desired x , i.e. until $x' = x$ is reached. Reflection high energy electron diffraction (RHEED) was used to monitor the growth mode and to calibrate the growth rates of GaAs and $\text{In}_x\text{Ga}_{1-x}\text{As}$ and hence to determine the InAs molar fractions x . The other growth conditions are described in detail elsewhere.^[13]

Temperature dependent electron mobilities were measured by resistivity and Hall effect measurements from 300 K down to 1.6 K on six-arm Hall bars prepared by photolithography and lift-off procedures. The orientation dependence of electron mobility was studied by aligning the Hall-bars such that the current density vector is parallel to the two orthogonal $\langle 110 \rangle$ directions separately. Double-crystal x-ray diffraction, and in some cases electron transmission microscopy (TEM) were used to characterize the structural properties of the specimens.

RESULTS AND DISCUSSION

Fig. 1 shows the temperature dependent electron mobilities of 2DEG in lattice matched $\text{In}_y\text{Al}_{1-y}\text{As}/\text{In}_x\text{Ga}_{1-x}\text{As}$ ($x < 0.4$) MD heterojunctions in the two orthogonal $\langle 110 \rangle$ directions. At room temperature, the electron mobility μ is about $9 \times 10^3 \text{ cm}^2/\text{V-s}$ and nearly independent of orientation and composition. In the range of $50 \text{ K} < T < 300 \text{ K}$, μ increases with decreasing temperature, showing a $T^{-\alpha}$ dependence with $1.0 < \alpha < 1.5$. For $T < 50 \text{ K}$, the mobilities are almost independent of temperature, but decrease with increasing InAs molar fraction x . The average values of μ at 77 K are from $3.8 \times 10^4 \text{ cm}^2/\text{V-s}$ for $x = 0.2$ to $2.5 \times 10^4 \text{ cm}^2/\text{V-s}$ for $x = 0.4$. The corresponding 2-D electron concentrations (n_s) are 7.8×10^{11} to $1.3 \times 10^{12} \text{ cm}^{-2}$. Such composition dependence of electron mobility is believed to be primarily due to increasing alloy scattering.^[12] For comparison, the values of μ reported of pseudomorphic $\text{In}_x\text{Ga}_{1-x}\text{As}$ MD heterostructures in the same composition range^{[14]-[16]} are between 1×10^4 and $2 \times 10^4 \text{ cm}^2/\text{V-s}$ at 77 K.

The orientation dependence of μ is most evident at low temperature as seen in Fig. 1. The highest electron mobilities are always found in the $[1\bar{1}0]$ orientation and the lowest in the orthogonal $[110]$ direction. In this paper, $[1\bar{1}0]$ orientation is referred to the direction

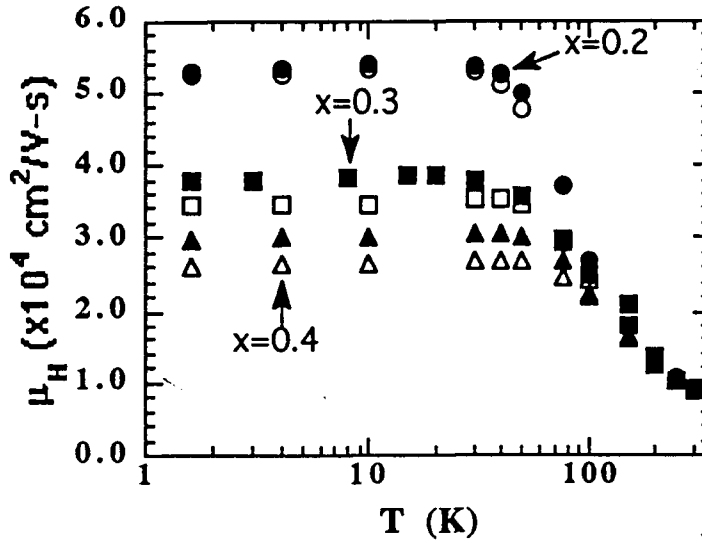


Fig.1. Temperature dependent electron mobility of 2DEG in strain relaxed, lattice matched $\text{In}_y\text{Al}_{1-y}\text{As}/\text{In}_x\text{Ga}_{1-x}\text{As}$ MD heterojunctions. The circles are for $x=0.2$, squares for $x=0.3$, and triangles for $x=0.4$. The solid symbols represent data in $[\bar{1}10]$ orientation and open symbols in $[110]$ direction.

perpendicular to the major flat of the 2-inch diameter wafers. The percentage anisotropy of low temperature electron mobility, defined as $\Delta\mu/\mu[\bar{1}10] = (\mu[\bar{1}10] - \mu[110])/\mu[\bar{1}10]$ is found to increase with x . Negligible anisotropy in n_s was observed. These results are summarized in Table I. It should be pointed out that the $\langle 110 \rangle$ orientation dependence of μ is not due to the lattice mis-orientation created by the 2° offcut of the substrate, because the axis of the offcut is 45° to the orthogonal $\langle 110 \rangle$ directions.

Table I. Electron mobilities of 2DEG in the $\text{In}_y\text{Al}_{1-y}\text{As}/\text{In}_x\text{Ga}_{1-x}\text{As}$ MD heterojunctions at 300 K and 1.6 K obtained by resistivity and Hall effect measurements in the orthogonal $\langle 110 \rangle$ orientations. The fractional anisotropies $\Delta\mu/\mu[\bar{1}10]$ are also listed for different x .

sample ID	x	Electron mobility ($\text{cm}^2/\text{V-s}$)				$\Delta\mu/\mu[\bar{1}10]$	
		300 K		1.6 K		300 K	1.6 K
		$[\bar{1}10]$	$[110]$	$[\bar{1}10]$	$[110]$		
1922	0.2	8980	8850	53040	52480	1.4%	1.1%
1814	0.3	9340	8990	37840	34540	3.7%	8.7%
1923	0.3	9400	8860	41050	40530	0.7%	1.3%
1906	0.4	8900	8800	29920	26230	0.9%	12.3%
2009	0.4	8280	8230	24500	21890	0.6%	10.7%
1884	0.4	9870	8530	33860	22960	13.6%	32.2%

The electron mobility anisotropic is likely to depend on and to be correlated to the structural properties of these samples. A TEM study^[17] of an $x=0.3$ sample found that most of the dislocations are formed and confined to the buffer layers at the interfaces between steps. The top $\text{In}_{0.3}\text{Ga}_{0.7}\text{As}$ layer had fewer than $10^6/\text{cm}^2$ threading dislocations. In addition, a small number of misfit dislocations ($\sim 1 \times 10^4 \text{ cm}^{-1}$) are seen lying in the $[\bar{1}10]$ direction; no dislocation running along $[110]$ orientation near the electron conduction channel at the $\text{In}_{0.29}\text{Al}_{0.71}\text{As}/\text{In}_{0.3}\text{Ga}_{0.7}\text{As}$ interface. At the $\text{In}_{0.3}\text{Ga}_{0.7}\text{As}/\text{In}_{0.2}\text{Ga}_{0.8}\text{As}$ interface, asymmetric misfit dislocation densities of $2.0 \times 10^5 \text{ cm}^{-1}$ and $1.6 \times 10^5 \text{ cm}^{-1}$ are observed for $[\bar{1}10]$ and $[110]$ orientations respectively. The extent of strain relaxation of the structure was measured using X-ray rocking curves from both (004) and (224) diffractions.^[17] Asymmetric strain relaxation was observed together with a large tilt of each epilayer about the $[\bar{1}10]$ in plane axis. For the $x=0.3$ epilayer, the total misfit strain, $\Delta a/a_s=0.021$ relative to the substrate, was relieved by 85% in the $[\bar{1}10]$ orientation and by 98% in the $[110]$ direction. The amount of strain relieved was consistent with the observed dislocation densities. In addition, the epilayers were tilted relative to the GaAs substrate with the tilt axis parallel to the $[\bar{1}10]$ direction.^[17] The tilt angle was found to increase with x , i.e. with the total misfit strain. The origin of the structural anisotropy of strain relaxed $\text{In}_x\text{Ga}_{1-x}\text{As}$ grown on GaAs is not well understood, but likely involves differences in α , β dislocation mobilities^[18] and effect of the substrate offcut angle on the tetragonal strain at the interface.^[19] A TEM study of the $x=0.4$ samples, however, revealed larger number of dislocations threading through the conduction channel.

The effect of dislocations on the electron mobility can be understood as two fold. Firstly, the piezoelectric potential produced by the long-range strain field of dislocations adds an extra electric field component which affects the electron momentum. The resultant reduction of electron mobility is orientation-dependent because the charge density associated with the piezoelectric effect is anisotropic.^[20] Secondly, dislocations act as 'acceptor'-like trapping centers as first suggested by Read^[3]. They are neutral at room temperature but ionized at low temperatures. The Coulombic potential associated with these charged lines provides an additional anisotropic scattering mechanism for electrons. Dislocation scattering has been treated theoretically by several authors,^{[3],[4],[21],[22]} and anisotropic electron mobilities were predicted. Another general conclusion is that for misfit dislocation density less than 10^5 cm^{-1} their effect is not significant.^[5] Zhao et al.^[22] showed that for misfit dislocation density of $1 \times 10^4 \text{ cm}^{-1}$, the electron mobility μ_D limited by dislocation scattering is in the order of $10^5 \text{ cm}^2/\text{V-s}$. In our $x=0.3$ sample, since the misfit dislocations are only running along $[\bar{1}10]$ orientation at the channel, we can assume that the electron mobility μ is only affected in $[110]$ direction and estimate μ_D , using Matthiessen's rule, $\mu^{-1} = \Sigma \mu_i^{-1}$. It is then found that $\mu_D \sim 4 \times 10^5 \text{ cm}^2/\text{V-s}$, in qualitative agreement with the calculation by Zhao et al.^[22]

A comparison of μ for strain relaxed $\text{In}_{0.15}\text{Al}_{0.85}\text{As}/\text{In}_{0.17}\text{Ga}_{0.83}\text{As}$ and pseudomorphic $\text{Al}_{0.35}\text{Ga}_{0.65}\text{As}/\text{In}_{0.17}\text{Ga}_{0.83}\text{As}$ heterojunctions showed much higher electron mobilities of strain relaxed structures, averaging $7.25 \times 10^4 \text{ cm}^2/\text{V-s}$, compared to $5.28 \times 10^4 \text{ cm}^2/\text{V-s}$ of the pseudomorphic structures with a comparable anisotropy as seen in Table II. Reported data of 'quasi' pseudomorphic structures by Sun et al.^[11] and by Webb et al.^[7] are also listed in Table II for comparison with those listed in Table I. Again, the strain relaxed structures have higher average mobilities. A plot (Fig. 2) of electron mobility anisotropy $\Delta\mu/\mu_{[\bar{1}10]}$ versus InAs molar fraction x shows a smaller anisotropy for the strain relaxed structures in the comparable composition range. These results provide additional evidence of the good crystalline quality of

Table II. Comparison of electron mobilities and anisotropy for strain relaxed (#2013) and pseudomorphic (#1989) $\text{In}_{0.17}\text{Ga}_{0.83}\text{As}$ heterostructures. Data of Webb et al.[7] and Sun et al.[11] are also listed for comparison.

sample ID	x	well thickness (nm)	Electron mobility ($\text{cm}^2/\text{V-s}$)				$\Delta\mu/\mu_{[\bar{1}10]}$	
			300 K		Low Temp.		300 K	Low T
			$[\bar{1}10]$	$[110]$	$[\bar{1}10]$	$[110]$		
2013	0.17	300	10000	10430	76110	68970	-3.6%	9.4%
1989	0.17	10	9300	9440	55070	50490	-2%	8.3%
<hr/>								
L5-2° a	0.04	300	4250	2750	50000	42700	35%	14.5%
L6-2° a	0.10	300	10700	6900	82000	62500	36%	24%
L7-2° a	0.15	300	8700	4100	59500	41000	53%	31%
L8-2° a	0.20	300	4300	2100	19600	17900	51%	8.7%
TH369b	0.15	12	7360	7070	35200	29800	3.9%	15%
TH366b	0.15	15	7270	7060	34700	30200	2.9%	13%
TH368b	0.15	20	7100	5930	24800	14300	16.5%	42%
TH367b	0.15	25	6600	6750	16800	23900	-2.3%	-30%
TH370b	0.15	30	6500	5130	24300	14900	21%	39%

a. From ref. 11. The low temperature data were taken at 60 K.

b. From ref. 7. The low temperature data were taken at 77 K.

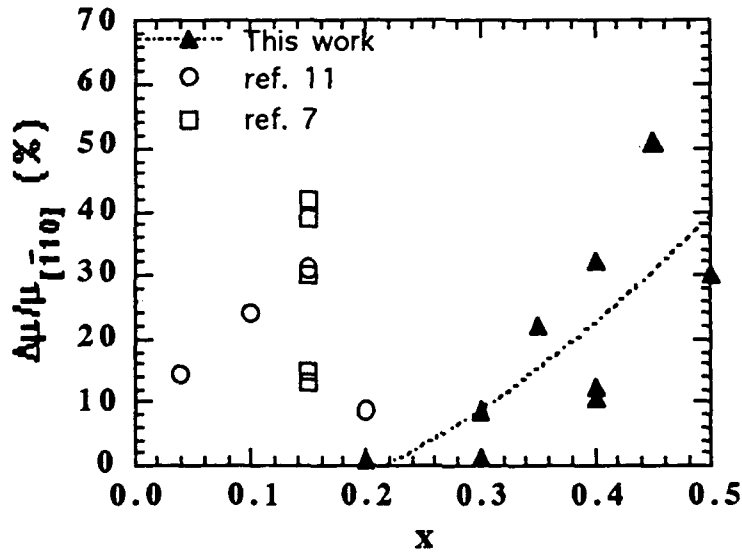


Fig.2 Electron mobility anisotropy $\Delta\mu/\mu_{[\bar{1}10]}$ versus InAs molar fraction x of this work (triangles) and Webb et al.[7] and Sun et al.[11] The dashed curve is a guide to the eye.

our samples and also indicate that the effect of dislocations on the transport properties of 2DEG may not be significant in properly grown strain relaxed structures despite the fact that strain relaxation involves the formation of large numbers of dislocations, provided that the conduction channel is kept far away from majority of the dislocations.

SUMMARY

We have studied the transport properties of two-dimensional-electron-gas in strain relaxed $\text{In}_y\text{Al}_{1-y}\text{As}/\text{In}_x\text{Ga}_{1-x}\text{As}$ ($x < 0.4$) using resistivity-Hall effect measurements. A $\langle 110 \rangle$ orientation dependent anisotropy in electron mobility was observed at low temperatures and attributed to the effect of dislocations and to their asymmetric distribution. The effectiveness of a compositionally step graded buffer providing strain relaxation and acting as a dislocation filter is demonstrated by the measurement of higher electron mobilities and smaller anisotropy of 2DEG in the heterojunctions grown on such buffers compared to those of 'quasi' pseudomorphic structures. The strain relaxed heterostructures may be advantageous for device applications because majority of the dislocations can be constrained to remain far from the electron conduction channels.

ACKNOWLEDGEMENT

The authors acknowledge the financial support for this work provided by the Naval Research Laboratory and offer their thanks to Professor K.L. Kavanagh and J.C.P. Chang for providing some of the structural data and for many useful discussions.

REFERENCES

1. I.J. Fritz, S.T. Picraux, L.R. Dawson, T.J. Drummond, W.D. Laidig, and N.G. Anderson, *Appl. Phys. Lett.* 46, 967 (1985)
2. I.J. Fritz, P.L. Gourley, and L.R. Dawson, *Appl. Phys. Lett.* 51, 1004 (1987)
3. W.T. Read, *Phil. Mag.* 46, 111 (1954)
4. C.M. Penchina, J.L. Farvaque, and R. Marut, *J. Appl. Phys.* 53, 4970 (1982)
5. R.A. Logan, G.L. Pearson, and D.A. Kleinman, *J. Appl. Phys.* 30, 885 (1959)
6. J.J. Duga, *J. Appl. Phys.* 33, 169 (1962)
7. C. Webb, J.N. Eckstein, and Y.M. Desai, *J. Cryst. Growth* 111, 309 (1991)
8. Q. Sun, D. Morris, C. Lacelle, and A.P. Roth, *Mater. Res. Soc. Proc.* 160, 783 (1989)
9. T. Schweizer, K. Kohler, W. Rothmund, and P. Ganser, *Appl. Phys. Lett.* 59, 2737 (1991)
10. S.R. Bahl, W.J. Azzam, and J. A. del Alamo, *J. Cryst. Growth* 111, 479 (1991)
11. Q. Sun, C. Lacelle, D. Morris, M. Buchanan, P. Marshall, P. Chow-Chong, and A.P. Roth, *Appl. Phys. Lett.* 59, 1359 (1991)
12. Jianhui Chen, J.M. Fernandez, and H.H. Wieder, *Appl. Phys. Lett.*, 1992 to be published.
13. Jianhui Chen, J.M. Fernandez, J.C.P. Chang, K.L. Kavanagh, and H.H. Wieder, *Semicon. Sci. Technol.* 7, 601 (1992)
14. W.C. Hsu, C.M. Chen, and W. Lin, *J. Appl. Phys.* 70, 4332 (1991)
15. M.V. Baeta Moreira, M.A. Py, M. Gailhanou, and M. Illegems, *J. Vac. Sci. Technol. B* 10, 103 (1992)
16. K. Inoue, K. Nishii, T. Matsuno, and T. Onuma, *IEDM Tech. Digest* 1987, p422